FINITE ELEMENT ANALYSIS OF SOFT ROBOTIC GRIPPER FOR PINEAPPLE HARVESTING

BY

SUMITH S RAJU (2020-02-014)

JUSTIN BASIL ISAC (2020-02-019)

SOORYA SURENDRAN (2020-02-025)

AFNA SHARIN E P (2020-02-031)

KERALA AGRICULTURAL UNIVERSITY

DEPARTMENT OF FARM MACHINERY AND POWER ENGINEERING

KELAPPAJI COLLEGE OF AGRICULTURAL ENGINEERING AND TECHNOLOGY

TAVANUR- 679573, MALAPPURAM

KERALA, INDIA

2024

FINITE ELEMENT ANALYSIS OF SOFT ROBOTIC GRIPPER FOR PINEAPPLE HARVESTING

BY

SUMITH S RAJU (2020-02-014)

JUSTIN BASIL ISAC (2020-02-019)

SOORYA SURENDRAN (2020-02-025)

AFNA SHARIN E P (2020-02-031)

PROJECT REPORT

Submitted in partial fulfillment of the requirement for the degree of Bachelor of Technology

in

Agricultural Engineering

Faculty of Agricultural Engineering and Technology

KERALA AGRICULTURAL UNIVERSITY

DEPARTMENT OF FARM MACHINERY AND POWER ENGINEERING

KELAPPAJI COLLEGE OF AGRICULTURAL ENGINEERING AND TECHNOLOGY

TAVANUR-679573, MALAPPURAM

KERALA , INDIA

2024

DECLARATION

We, hereby declare that this report entitles **"FINITE ELEMENT ANALYSIS OF SOFT ROBOTIC GRIPPER FOR PINEAPPLE HARVESTING"** is a bonafide record of research work done by us during the course of B.Tech and this report has not previously formed the basis for the award to us of any degree, diploma, associateship, fellowship or other similar title, of any other university or society.

Place: Tavanur

Date:

Sumith S Raju (2020-02-014)

Justin Basil Isac (2020-02-019)

Soorya Surendran (2020-02-025)

Afna Sharin E P (2020-02-031)

CERTIFICATE

Certified that this report entitled "**FINITE ELEMENT ANALYSIS OF SOFT ROBOTIC GRIPPER FOR PINEAPPLE HARVESTING**" is a record of research work done independently by Mr. Sumith S Raju, Mr. Justin Basil Isac, Ms. Soorya Surendran, Ms. Afna Sharin E P under my guidance and supervision and that it has not previously formed the basis for the award of any degree, diploma, fellowship or associateship to them.

Place: Tavanur

Date:

Er. Sindhu Bhaskar
(Project Guide)
Assistant Professor & PI
AICRP on FIM
KCAET, Tavanur

Dr. Edwin Benjamin
(Project Guide)
Assistant Professor(C),
Dept. of FMPE,
KCAET, Tavanur

ACKNOWLEDGEMENT

We would like to express our gratitude and appreciation to all those who gave us the opportunity to complete the project.

We express our special thanks to our project guide **Er. Sindhu Bhaskar**, Assistant Professor & PI, AICRP on FIM, KCAET Tavanur, for her dynamic and valuable guidance, care, patience and keen interest in our project work. We consider it as our greatest fortune to have her as the guide for our project work and our obligation to her lasts forever.

This would be the right moment to thank **Dr. Jayan P.R**, Dean of faculty, Professor and Head, Dept. of FMPE, KCAET Tavanur, for his support during the course of the project work.

We also extend our sincere thanks to **Dr. Edwin Benjamin (**Project Guide) Assistant Professor(C), Dept. of FMPE, KCAET Tavanur, for the guidance, encouragement and support throughout the project.

We would also like to express our sincere gratitude to **Er. Vishnu Prasad S R,** Assistant Engineer (D/W), FMTC, KCAET Tavanur, for his help and information sharing along the project.

We would like to thank **Er. Ranjisha K,** for her invaluable help, creative ideas, and wise counsel over the course of our project.

We would like to express our gratitude to **Mr. Agnesh Kumar**, Application Engineer, KAIZANET Technologies PVT LTD, for his instruction in Ansys software.

We express our sincere thanks and gratitude to Kerala Agricultural University for providing this opportunity to do the project work.

We also thank all the teachers, technical staffs, office staffs for their support and co-operations.

We wish to remember and delight our parents who always bless us for our betterment and pray for our success.

We also express my ineffable and glowing gratitude to our friends and classmates for their helping hands for fulfilment of this great venture.

We also acknowledge All India Co-ordinated Research Project (AICRP) for technically supporting us in completing our project work.

We would like to thank everyone who has assisted us in any way during the course of this project.

DEDICATED TO OUR PROFESSION

TABLE OF CONTENTS

LIST OF TABLES

LIST OF FIGURES

LIST OF PLATES

SYMBOLS AND ABBREVIATIONS

Abbreviation/Notation	Description
×	Multiply
°	Degree
cm	Centi meter
FEA	Finite Element Analysis
FEM	Finite Element Method
KCAET	Kelappaji College of Agricultural Engineering and Technology
kg	Kilogram
$kg.m^{-3}$	Kilogram per meter cube
kPa	Kilo Pascal
mm	Millimeter
$N.cm^{-2}$	Newtons per square centi meter
SPA	Soft Pneumatic Actuator
CAD	Computer-Aided Design
FDM	Fused Deposition Modeling
ANOVA	Analysis of variance
SH	Self-healing
LCD	Liquid-crystal display
SRF	Soft Robotic Fingers
SMA	Shape Memory Alloys
DC	Direct Current
PWM	Pulse Width Modulation
FPN	Fast pneu-nets
SPN	Slow pneu-nets
SMA	Shape Memory Alloys
MR	Magnetorheological
SMRE	Shape-adaptive Magnetorheological Elastomers

Introduction

CHAPTER I

INTRODUCTION

The pineapple (Ananas Comosus) is one of the most valuable commercial fruits in the world. Harvesting of pineapple is a major operation in pineapple cultivation and is laborious, and energy-intensive involving 306 man-hours per acre approximately. Manual harvesting by sickle is always injury-prone, which reduces the harvesting efficiency because the pineapple consists of long-pointed leaves usually needle-tipped and generally bearing sharp, up-curved spines on the margins (Singh *et al*., 2022).

Pineapple is one of the most important tropical fruit grown in India. India is the fifth largest producer of pineapple with annual output of about 1.2 millions. In spite of having numerous developments in the field of food processing most of the fruits grown is not getting processed which leads to post harvest losses. Ultimately this leads to less revenue for farmers in turn of their investment. So, there is a need to make cultivators aware of recent developments in the field of pineapple harvesting (Saloni *et al*., 2017). Pineapple grown in the Vazhakkulam village of Eranakulam district of Kerala has got Geographical Indication tag and hence the village is known as Pineapple City. April – May and August – September are the commending season for pineapple cultivation in Kerala (KAU, 2016). Moreover, "Mauritius Pineapple" variety is being cultivated in Kerala. It has got high demand as a fresh fruit throughout India and also foreign countries because of its quality, sweetness and good flavour. In Kerala the annual production of pineapples were around 69000 tonnes (Thomas and Dinesh, 2020).

Harvesting operation of pineapple exposes the workers to several health hazards such as body strain due to awkward posture and repetition. Exposure to harsh environmental conditions results in musculoskeletal symptoms (MSS) and ergonomic risks (Singh, 2020). In such a condition, an automatic harvesting equipment for pineapple will be helpful for alleviating labour shortages, lightening labour intensity, improving picking efficiency, reducing production cost. Designing

an end-effector for pineapple is one of the key problems faced while developing automatic pineapple harvesting equipment. Apart from harvesting, end actuator can also be used for postharvest operations like sorting, grading etc.

Agriculture 4.0 presents several challenges for the automation of various operations, including the fundamental task of harvesting. One of the crucial aspects in the automatic harvesting of high value crops is the grip and detachment of delicate fruits without spoiling them or interfering with the environment. Soft robotic systems, particularly soft grippers, offer a promising solution for this problem, as they can operate in unstructured environments, manipulate objects delicately, and interact safely with humans (Navas *et al*., 2024).

Soft grippers integrate under-actuation and compliance by replacing rigid joints with a structure made of hyper-elastic materials that deform continuously in response to external or internal actuators and to the interaction with the objects. Compliant materials thus play a key role in soft grippers: material characteristics such as maximum elastic deformation, stiffness and viscoelasticity influence the stroke of the gripper, the force it can generate, and its response time. The most widely used materials for soft grippers are elastomers (Shintake *et al*., 2018).

Soft gripper has been developed using design/ CAD software – SolidWorks. Soft Pneumatic Actuators (SPAs) are the most common and widely utilized soft actuators. SPAs are fabricated using elastomeric (hyper-elastic) materials. SPA actuates under increasing pressure and creates the required bending configuration. The SPAs with corrugated structures create high bending angles and experience minimum stress even at low actuating pressure. SPAs are having chambers for pneumatic actuation. SPAs produce bending on the application of pneumatic pressure. SPAs are made up of hyper-elastic or rubber-like material, such as silicon rubber. The stress-strain relationship of a hyper-elastic material is nonlinear and defined by using the strain energy density function. The strain energy density or potential defines the strain energy stored in the material per unit volume as a function of strain at that point in the material. Generally, hyper-elastic or rubber-like materials are considered isotropic materials having similar properties in all

directions. They are subjected to very large deformation than their original length, for which hyper-elastic material models analysed using the Finite Element Method (FEM) are required. FEM is a very good tool for predicting the bending behaviour and stress distribution of the soft actuators. The simulation of the soft pneumatic actuator is carried out using the FEM (Ansys WB R2) technique (Gariya *et al*., 2022).

The project has been carried out to develop a soft robotic pineapple gripper with the following objectives.

- To study fruit parameters towards the development of soft robotic pineapple grippers.
- To design soft robotic pineapple gripper using CAD software.
- To optimise material and geometry of soft robotic pineapple gripper using FEM analysis.

Review of literature

CHAPTER II

REVIEW OF LITERATURE

Brief review of the works done relevant to different aspects of this research, which include study of physical and mechanical properties of pineapple, design and Finite Element Analysis of soft robotic pineapple gripper, are explained in this chapter.

2.1 PHYSICAL AND MECHANICAL PROPERTIES OF PINEAPPLE

Physical and mechanical properties of pineapple such as shape, top diameter, bottom diameter, middle diameter, length of pineapple, weight of pineapple and firmness of pineapple were measured. Research articles that mention the measurement of these properties are described briefly here.

Valente *et al*., (2001) conducted non-destructive evaluation of firmness of pineapple by acoustic impulse method. A steel ball with a diameter of 10 mm that was dropped from a height of 500 mm made to strike a fruit, or a hand-held wooden rod with a diameter of 10 mm and a length of 180 mm was used for the same purpose, this creates an acoustic response and the greatest resonant frequency thus obtained from the fruit used for the estimation of acoustic firmness and the elasticity coefficient derived from acoustic measurements holds promise as a non-destructive method for assessing overall pineapple firmness.

Pathaveerat *et al*., (2008) evaluated a variety of physical and chemical criteria for categorizing pineapple according to maturity or the existence of marbling defects. They tested 120 sample pineapples from the "Pattavia" cultivar, which were then divided into three groups based on their varying levels of maturity based on the translucent yellow area of the longitudinal cut-open surface, and a further group consisting of marbled fruit. Compression test is used to measure the destructive parameters which include flesh firmness, titratable acidity and soluble solids content. Each sample was subjected to non-destructive measuring methods,

such as acoustic impulse response tests and the determination of specific gravity using water replacement.

Xia *et al*., (2012) measured weight, shape and size of 30 Guangdong's pineapple samples, vertical height covers from 98.4 mm to 113.7 mm, top diameter was from 63.1 mm to 85.2 mm, bottom diameter ranges from 74.6 mm to 93.8 mm, transverse diameter was about 106.2 mm to 173.5 mm, and weight was from 0.725 kg to 1.515 kg. Transverse diameter was taken as design factor. Characteristics of static load extrusion mechanics was tested. The limit compression strengths of the pineapple were from 0.146 MPa to 0.243 MPa and the extruding limit loads of were from 0.533 kN to 0.887 kN.

2.2 DESIGN AND DEVELOPMENT OF SOFT ROBOTIC GRIPPERS

A soft robotic pineapple gripper primarily consists of soft gripper and pneumatic actuation unit. This section includes a brief explanation of previous research on pineapple picking grippers, soft grippers, different actuation technologies and material and geometry optimisation of soft grippers.

2.2.1 Pineapple picking gripper

Wang *et al*., (2012) designed a typical manipulator for pineapple harvester and its control system. The designed manipulator consists of three parts, the rotating mechanism, the manipulator driving mechanism and the grabbing mechanism. Grabbing mechanism consists of double pivots rotating gripper which can perform grabbing and holding actions on pineapples. It consists of base plate, two fingers, driving bar, two handles, pin and two L bars. Fingers are separately fixed on the handles which are hinged by bolts for the rotation motion to separate pineapple from the plant. Test results showed that, when the grabbing mechanism rotates at 180°, pineapples can be steadily grasped and harvested, the average harvesting time was 23 s.

Xia *et al*., (2012) studied about the design of end-actuator of Guangdong's Bali pineapple. Sliding-lever double-fulcrum structure is selected as the clamping mechanism. When its finger lever angle α takes 35°, v-shaped groove angle was

120°, the centre distance of the two fulcrum was 110 mm, finger lever length AB l takes 135 mm, thus satisfying the requirements for clamping error, and the optimized deflection angle β was 87.6°. Clamping force analysis showed that the designed picking end-actuator can ensure zero damage while harvesting the pineapple.

Salleh and Sukadarin (2018) reviewed the concept of human factor and ergonomics in pineapple plantations and the risk model. Ergonomic approach was aimed at how to make human activities more efficient, comfortable, satisfying, and safe. Also, to optimise human interactions with the systems. While human factor was a field concerned to deal with the design of systems in order to lessen human error and minimize ergonomics related issues. Results showed that prolonged psychological and physical exposures can affect the development of Work-related Musculoskeletal Disorders (WMSDs) such as knee pain and low back pain among the workers.

Zhang *et al*., (2018) designed a semi-automatic screw type pineapple picking-collecting machine according to the width between two ridges of the pineapple. The pineapple picking and collecting machine was composed of a moving part, a pineapple conveying part, a picking part, a pineapple collecting part, and a lifting part. Machine was portable, and can be easily operated. The harvester improves the production efficiency, reduces the physical labour degree of pineapple pickers, and can successfully fulfil the different flexible picking demands of small-scale pineapple farmers.

Anh *et al*., (2020) developed a pineapple harvesting robotic system that works autonomously. The system contains two robotic manipulators mounted on a platform, an image-based harvesting control unit, custom end-effectors and a machine vision unit. Each end-effector comprises a gripper for firmly holding the selected pineapple fruit and a saw-disc cutter for detaching the stalk. The gripper has two pieces forming to pineapple-shape cage. The open/close of the holding cage are operated by a pneumatic actuator. The experiment results show the success in the recognition of pineapple with 90.82 % mAP.

Kurbah et al. (2022) developed a three fingered gripper cum cutter for harvesting pineapple. CREO software is used for developing a model of the gripper. The gripper consists of three fingers. The parts are connected through pin joint to allow relative rotation motion between components to allow close and open of finger to hold and release the pineapple. These components are linked through strings which is connected to the shaft of a servo motor. The rotation of servo motor causes the operation of the fingers, which in turn helps in grasping. To obtain final design of the gripper component, mechanical analysis of the 3D printed gripper components has been done. FDM 3D printing manufacturing technique is used for the fabrication of gripper component. Finally, the working model was developed by assembling 3D printed gripper components.

2.2.2 Soft grippers

Manti *et al*., (2015) developed a bioinspired soft robotic gripper for effective grasping. The soft robotic gripper consists of three identical soft fingers that were connected to a rigid frame and were activated by a DC motor through a cable based under actuated mechanism. They considered two materials, Dragon Skin 30 and Smooth-Sil 950 and made three kinds of gripper, two using each material, one a combination of two material. Considering each of the grippers has similar weight, third model having a grasping force of 3.5 N was finalised.

Abd *et al*., (2017) conducted a study to investigate the impact that soft actuator taper angle has upon the force and displacement of the actuator. When changing the taper angle. Seven SPAs, each with a different taper angle ranging from 0° to 6° in 1° increments were designed in this article, while the other parameters were constant. Ecoflex 00-30 was the material used for fabrication. After performing 1-way Analysis of Variance (ANOVA) analysis they found that the force output by the actuator with a taper angle of 2° produced the largest force, whereas the actuator with a taper angle of 6° produced the most displacement in unconstrained tests.

Ongaro *et al*., (2017) reported the potential of soft, untethered grippers in tasks that involve autonomous manipulation, as well as obstacle recognition and manipulation in unstructured environments. Two experiments were performed for this purpose. In the first, soft bilayer grippers were used to perform the pick-and place of soft irregularly-shaped biological material in the presence of both static and dynamic obstacles. The second experiment demonstrates that soft grippers can autonomously recognize, classify, and manipulate regularly-shaped micro-scale rigid objects. It is inferred that grippers were capable of completing pick-and-place tasks of biological material at an average velocity of 1.8 ±0.71 mm/s and a drop-off error of 0.62 ±0.22 mm. Colour-sensitive sorting of three micro-scale objects was completed at a velocity of 1.21 ±0.68 mm/s and a drop-off error of 0.85 ±0.41 mm.

Terryn *et al*., (2017) studied on the problem of causing damage to the soft gripper by incorporating self-healing (SH) soft materials like SH concrete and SH asphalt. They intended to illustrate and describe the SH ability of DA (Diels-Alder) polymer samples. Ecoflex 0030 having a young's modulus of 67 kPa was used as construction material. Four soft pneumatic actuator prototypes were constructed. The actuator was then deflated, and the macroscopic cut was sealed autonomously. After subjecting the actuator to a heating procedure in an oven at a maximum temperature of 80°C the damage was completely healed, and the actuator was again airtight.

Sinatra *et al*., (2019) developed a flexible nanofiber-reinforced soft actuator for robust grasping of gelatinous marine organisms. The designed grasping device was composed of six fingers (composite actuator) connected to a three-dimensional (3D)–printed palm. They selected three design parameters which include interior channel height, thickness of the inflating membrane, and thickness of the adhesive layer. A prototype was fabricated and contact pressure exerted by individual actuator was quantified by operating it at a pressure of 6 psi (41.4 kPa), resulted average contact pressure was 0.0455 ± 0.007 kPa (mean ± SEM), which was less than the target of <1kpa.Gripper's region of acquisition, robustness of gripper to external forces were also evaluated.

Zhu *et al*., (2019) proposed a soft gripper for robust grasping. Double O-ring sealing mechanism was used to ensure system airtightness. Cross section of gripper was semi-circular of radius 10 mm, having nine inflation chambers. Finger bending angle tests were carried out to examine the finger's performance repeatability and reliability. With the aid of the integrated layer jamming unit, grasping robustness can be guaranteed when the robotic arm was moving at acceleration up to 8 m/s^2 Experimental results showed that the variable stiffness capacity was robust even in high acceleration.

Razif *et al*., (2020) developed a bellow shape soft gripper for agriculture application. A flex sensor was embedded in the soft actuator to measure the bending angle performance for the gripper and the angle values will be displayed on LCD. Then, the relationship between the air pressure supplied to the actuator and bending angle produced by the gripper was discussed. Experiment results shown that the bellow gripper could successfully grip and hold several types of fruits from 60 mm to 72 mm with the soft gripper perform the bending from 17 degrees to 23 degrees.

Kultongkham *et al*., (2021) developed a soft gripper for tomato harvesting with a force feedback system. The soft gripper consists of three fingers: each finger functions with the others through the connected controller and pneumatic regulator. The pneumatic regulator adjusts pressure and airflow through a normally-closed three-port solenoid valve. The direction of the airflow was controlled by Arduino controller and force sensors. Grasping test results showed that the tomato weighing 226-266 gm had grasped by applying a maximum holding pressure of 70 kPa. The maximum force on each finger proved to be 1.62 N, which was less than the tomato bio-yield of 2.57 N.

Lei *et al*., (2022) designed a multi-cavity pneumatic soft gripper, the shape of which was slender and similar to the arc. Besides, the cross section of the gripper was composed of nine nearly inverted, V-shaped, thin-walled network structure cavities in series. There was a ventilation channel at the bottom of the cavity, and the cavity was connected to a closed cavity by the limiting layer. Control and monitoring of the soft gripper are realized through the electrical control module, the

air circuit control module, and the sensor group module, and the size of the airflow velocity was controlled by PWM DC speed regulation. The adaptability of the soft gripper in grasping objects was verified. The results showed that the software gripper possesses good flexibility and can better grasp objects of different shapes.

Xiao *et al*., (2022) reported that soft grippers are an emerging field of robotics in recent years owing to their reduced control complexity, easy fabrication, and excellent compliance. However, the small contact area and force usually limit their grasping reliability. The grasping performance of the soft gripper is investigated experimentally. The results indicate that the grasp and pull-off force depend on the size and shape of objects and applied pressure. As the applied pressure is 60 kPa, the maximum grasp force and pull-off force reach 0.71 N and 8.15 N, respectively.

Wang *et al*., (2023*)* presented a fruit harvesting method that includes a novel soft robotic gripper and a detachment strategy to achieve apple harvesting in the natural orchard. The soft robotic gripper includes four tapered soft robotic fingers (SRF) and one multi-mode suction cup. The SRF is customised to avoid interference with obstacles during grasping, and its compliance and force exertion are comprehensively evaluated with FEA and experiments. The proposed robotic gripper is compact, compliant with apple grasping and generates a large grasping force. Finally validated in a natural orchard and achieves a detachment, damage and harvesting rate of 75.6%, 4.55%, and 70.77%, respectively.

2.2.2.1 Different Actuation Technologies

Different types of actuation technologies are there. It includes hydraulic actuation, pneumatic actuation, tendon-driven actuation, fluidic elastomer actuation, shape memory alloys etc. hence, brief explanation of previous research conducted on this area is discussed here.

Tolley *et al*., (2014) designed a composite robot with Pneu-Net architecture. The system includes controller board which functions to control the solenoid valves and small air compressors that actuate the soft robot. An ATmega168

microcontroller on the controller board consists of an Arduino bootloader for uploading, executing, and storing programs to control the soft robot. The Arduino interface was used for writing and uploading. They implemented an undulating gait that actuated the Pneumatic Networks of the robot in sequence and created an actuation wave that travelled through the body from the rear end towards the front end. This created a wave which in turn resulted in forward motion.

Mosadegh *et al*., (2014) reported three short comings of fabrication materials. They were slow actuation speed, large volume change and short lifespan. To get around these limitations they developed a novel pneu-net (pneumatic network) design. Also conducted a detailed comparison between fast pneu-nets (FPN) and slow pneu-nets (SPN) on design analysis, mass transport analysis, stress-strain analysis, rapid actuation and found that FPN was far better than SPN. They then investigated about the effect different dimensions have on the bending of FPNs also carried out fatigue tests of FPN. The result show that when inflated fully, the chambers of this new design experience only one-tenth the change in volume. This small change in volume requires comparably low levels of strain in the material at maximum amplitudes of actuation, and commensurately low rates of fatigue and failure.

Cianchetti *et al*., (2014) developed a bioinspired soft actuation system by using Shape Memory Alloys (SMA) springs combined with a flexible braided sleeve featuring a motor-driven cable and a conical shape. Transverse actuators were positioned inside the arm orthogonally to the direction of the arm's longitudinal axis, arranged in a square shape where as longitudinal actuators were positioned uniformly on the external surface of the arm. Grasping capabilities was assessed experimentally by working out several trials with objects with varying diameters and an ad hoc set-up is used to measure the force generated by the soft arm. The results showed that grasping the object at 50% of the length of the arm is effective for radii greater or equal to 17.5 mm.

Manti *et al*., (2015) developed a bioinspired soft robotic gripper for effective grasping. This soft robotic gripper consists of three identical soft fingers

that were connected to a rigid frame and were activated by a DC motor through a cable based under actuated mechanism. They considered two silicon materials, Smooth-Sil 950 and Dragon Skin 30 made three kinds of gripper, two using each material, one a combination of two material. Grasping posture, grasping force were experimentally tested. Considering each of the grippers has similar weight, third model having a grasping force of 3.5 N was finalised.

Shiva *et al*., (2016) conducted a study to develop Tendon-based stiffening, inspired from the muscles of octopus, for a soft manipulator actuated pneumatically. This robotic manipulator has two basic actuation types, intrinsic pneumatic actuation and extrinsic tendon-based actuation, inspiration from the antagonistic behaviour of the octopus arm. Experiments were carried out by applying an external force in different configurations while changing the stiffness by means of the two actuation mechanisms. Test results showed that dual, antagonistic actuation increases the load bearing capabilities for soft continuum manipulators and thus their range of applications.

Li *et al*., (2018) studied about untethered and pump-less autonomous soft robotics and developed 3-fingered pneumatic soft actuators. No connection tubes were required for air supply or release. Controlling was done by using a servo motor which was more accurate and much easier than controlling flow rate and air pressure. Actuator's characteristics like tendon pulling/releasing displacement D, tendon pulling/releasing speed V and tendon pulling force was measured. The precharged limiting pressure was kept below 0.1 MPa and therefore a maximum bending about 98º was obtained.

Shintake *et al*., (2018) conducted a review on soft robotic grippers. They categorized soft gripping into three technologies: actuation, controlled stiffness and controlled adhesion. Gripping by actuation consists of bending gripper fingers or elements around the object. Gripping using controlled stiffness destroys the huge change in rigidity of material combinations or some materials for holding an object. Gripping using controlled adhesion- variable stiffness- relies on surface forces at the interface between gripper and object. The results shows that gripping principles

reported here were demonstrated in air, and could also be used underwater, or even in vacuum. Pneumatic systems are particularly easy to adapt to different external pressures. Electroadhesion and dry adhesion work well in vacuum, but are not effective in liquid environments.

Navas *et al*., (2021a) designed a diaphragm-type actuators with three single channel embedded in a 3D printed hexagonal structure. The pneumatic system consists of an Abart Start O15 air compressor with a power of six litres and 1.1 kW, a pneumatic air treatment equipment, a pneumatic solenoid valve, a SMC ITV2050 electro-pneumatic regulator and a Honeywell 40 PC air pressure sensor. The contact force of these actuators were measured for various inflation pressures. The soft gripper then mounted on the dual-arm robotic harvester to assess the performance of the entire system and concluded that the soft gripper was able to successfully detach the detected fruits in 80 percent of the cases with a mean soft gripper actuation time of 1 s.

Terrile *et al*., (2021) compared two different soft gripper technologies, pneumatic actuation and electromechanical actuation by making four sample grippers. The first gripper was four fingered pneumatic gripper with fingers spaced around the centre of the gripper symmetrically. Operation of second pneumatic gripper was based on the jamming process made of an elastomeric plastic membrane filled with granular material. The experiment has been carried out in three different environments: normal, humid, and dusty to analyse the success rate for each environment. The results showed that the electromechanical gripper with passive structure and the pneumatic gripper with chambered fingers have highest success rate, with rates of 86% and 77% respectively.

Zaidi *et al*., (2021) discussed about the various actuation technologies for soft robotic grippers. It includes pneumatic actuation, vacuum actuation, cable-driven actuation, shape memory alloy actuation, electroactive polymer actuation, electro-adhesive actuation and some other types of actuations like electric actuators, HSA based actuators, using magnetorheological (MR) fluids, Shape-adaptive MR elastomers (SMRE) etc. Here it was inferred that the technologies including SMAs,

EAPs, and EA are still in a growing stage, and it will take time for them to be mature. However, they can be integrated with the pneumatic, vacuum, or cable-driven technologies such that a more efficient and reliable system could be developed.

2.2.2.2 Material and Geometry Optimisation

Studies conducted on different types of materials used for the development of soft gripper and their geometry are described here.

Brown *et al*., (2010) developed a universal robotic gripper based on the jamming of granular material. The gripper was made of a rubber bag (0.3 mm thick) with an average length of 40 mm that was 80 percent filled with smooth soda-lime glass spheres with a diameter of 100 mm. They performed pick-and-place operations to evaluate gripping performance, in which objects were lifted, moved and gripped. Here it was found that volume changes of less than 0.5% suffice to grip objects reliably and hold them with forces exceeding many times their weight.

Elsayed *et al*., (2014) designed a pneumatically actuating silicone module for robotic surgery applications. Three types of silicone materials, Dragonskin 0030, Ecoflex 0030 and Ecoflex 0050 were used and optimisation was done by finite element analysis (FEA). The geometry of a gripper module of 25 mm diameter and 65 mm length, 55 mm length of chamber, 3.7 mm radius of chamber, and 1.5 mm distance between the outer module surface and the chamber wall. The experimental study of the module showed that for an increase of the module diameter by 26 percent, there was larger ballooning effect.

Manti *et al*., (2015) developed a bioinspired soft robotic gripper for stable grabbing. They considered two types of soft silicon materials, Smooth-Sil 950 and Dragon Skin 30. Dragon Skin 30 silicone was bicomponent with a specific gravity of 1.08 g·cc $^{-}$1. The components were generally used with a mixing ratio of 1A:1B. Blue coloured Smooth-Sil 950 silicone with specific gravity of 1.24 g·cc $^{-1}$, was bicomponent (A&B) with a mixing ratio of 10A:1B. They fabricated three types of grippers, two using each material, one a combination of two material. Considering

each of the grippers has similar weight, third model having a grasping force of 3.5 N was finalised.

Wang and Hirai (2016) designed a dual mode 3D printed soft gripper. Four fingers were fabricated using two materials, DS 10 and DS 30. Each consists of twelve soft air chambers and a male interface. Among the twelve air chambers, one larger chamber has a wall thickness of 3 mm and the remaining eleven chambers have a wall thickness of 1.5 mm. On the bottom surface of the cover 2, a rippled structure was added to improve gripping stability and also to imitate a fingerprint. The finger's soft portion measures 86 mm in length. For the insertion of the air hose, a 4mm hole was made through the male interface. Grasping tests showed gripper fabricated with softer materials (DS 10) is more energy efficient for grasping but the maximum grasping weight is lower than that fabricated with a harder material (DS 30).

Abd *et al*., (2017) used SolidWorks 2015 to modify the molds to create actuators. The top and bottom pieces were assembled to hold the Ecoflex 00- 30 once the 3D printing process was complete. Ecoflex 00-30, which has a Shore hardness of 30 and young's modulus of 0.1 MPa, was the material used to fabricate the soft actuators. The study includes 7 models with taper angle θ varying from 0° to 6^{o} with 1^{o} increments, all other geometric parameters were constant. The actuators were tested at the frequency of 0.5 rad/s to obtain the maximum force. It was found that highest force applied by the tip of the soft actuator occurs with taper angle of 2^{o}.

Bernadi *et al*., (2017) conducted a mechanical analysis on silicone-based elastomers. They selected 5 types of silicon elastomers which includes two PDMS (Dow Corning, Sylgard 186 and Sylgard 184) and 3 RTV elastomers (Blue Stars Silicones, RTV 4420, RTV 4528 and SMI G/G 0.020”). Results showed that stiffness’s of these materials traverse a huge range from kPa to MPa which include the properties of materials used for biomedical devices, soft implants as well as dynamic bioreactors. SMI and PDMS Sylgard 184 were the stiffest materials,

PDMS Sylgard 186 and RTV 4420 were in between and RTV 4528 was the most compliant.

Terryn *et al*., (2017) carried out research to rectify the problem of causing damage to the soft gripper by incorporating synthetic self-healing (SH) soft materials named SH polymers like SH concrete and SH asphalt. They intended to illustrate the self-healing ability of DA (Diels-Alder) polymer samples (a diene and a dienophile). Ecoflex 0030 having a young's modulus of 67 kPa was used as construction material. The maximum bending angle can be achieved was 70º at a pressure of 25 kPa. Corresponding force was measured to be about 0.25 and 0.32N.

Gariya *et al*., (2022) designed and analysed a SPA considering three different hyper-elastic materials namely, Dragon Skin 30, Elastosil M4601, and Smooth-Sil 950. The obtained FEM results for the three soft/hyper-elastic materials are compared in terms of bending angle and stress distribution. It is found that, soft corrugated actuator developed with Dragon Skin 30 material generates maximum bending angle and is subjected to least stresses as compared to the other two materials.

Jiao *et al*., (2022) put forward a novel idea of making dual-mode light weighted soft actuator using foam material and bellows. A foam actuator was designed with a negative pressure pneumatic drive comprising bellows air chambers, a polyurethane foam body, and sealing layers at the head and tail. Experiments were performed to test the bending and contraction performances of the actuator with the foaming multiplier and air chamber length as variables. At air pressures of 0–90 kPa, the bending angle and contraction of the actuator increased with the foaming multiplier and number of air chamber sections. The designed actuator achieved a bending angle of 56.2° and contraction distance of 34 mm (47.9% of the total length) at 90 kPa, and the bending and contraction output forces were 3.5 and 7.2 N, respectively.

2.2.2.3 Finite element analysis

Hu *et al*., (2018) investigated the effects of various design parameters on the actuation performance of a pneumatic network actuator (PNA), optimise its structure using the finite element method (FEM. The effects of the structural parameters, including the operation pressure, the wall thickness and the gap between the chambers, bottom layer thickness, and the geometry of the channel cross section, on the deformation and bending angle of the actuator were evaluated to optimise the performance of the pneumatic actuator. After the parameter optimisation, a pneumatic channel with a 4.5 mm bottom layer thickness, 1.5 mm wall thickness, and 1.5 mm gap between sequential chambers is recommended to perform optimised bending motion for the pneumatic network actuator.

Lei *et al*., (2022) conducted an analysis on the bending deformation of a soft gripper under input pressure. ABAQUS finite element software was used to model the soft gripper of the soft robot in a specific environment. In addition, the calculation and analysis were carried out on the thickness of the air cavity of the soft gripper, the distance between adjacent air cavities, the height of the air cavity, the number of air cavities, and the thickness of the bottom. Through the simulation analysis of the bending deformation factors of the soft gripper. Through simulation, it is analysed that the soft gripper was bent and deformed by changing the air pressure in the cavity to improve the load capacity of the gripper.

Gariya *et al*., (2023) focused on the analytical modelling of a SPA for analysing its bending behaviour under application of the input pneumatic pressure. The estimated bending results of the analytical model are compared and verified with the numerical method i.e., Finite Element Analysis (FEA). The bending results obtained from the analytical model showed high error when compared with the FEA results. Therefore, in this work, the analytical model is modified by using a linear correction term in the model. As a result of that, the error between the analytical and the numerical methods is significantly reduced.

Wang *et al*., (2023) conducted a simulation in Abaqus/CAE with the material properties. The SRF, block, and apple are imported into the Abaqus in step format. Then the material properties are assigned for each object. The SRF, block and apple are meshed with tetrahedral quadratic hybrid elements (element type C3D10H) for faster convergence. SRF and block, is then created to find the blocked tip force of the SRF. The tip force increases with the increases of inflation pressures. Here it was inferred that the maximum tip force is under 140 kPa inflation pressure when the distance equals 0 mm.

Riady and Evans (2024) investigates the gripping stress and deformation of pneumatically actuated fluidic elastomer actuation based soft robotic gripper through ansys finite element analysis software. By varying gripper parameters, i.e. input pressures and clearance to the object, simulations on the deformation of the soft fingers are performed to achieve gripping of the object. The experimental setup consists of the soft gripper, a base plate and a spherical work piece that is selected as the gripped object. Overall dimension of the finger is 62 mm (L) x 20 m (W) x 25 mm (H) and 1 mm wall thickness. The base thickness is 5 mm. Each finger contains an arched end with a 30 mm radius, and bellow-type ribs along the finger. The chosen material is silicone rubber of grade KE-575-U. It concluded that once the fingers make contact with the ball, the average total deformations of the fingers increase with higher clearance ratios and finger spacings. Furthermore, a gripper with a larger finger spacing develops more equivalent stress for a given input pressure than a gripper with a smaller finger spacing. The finger's average equivalent stress is 104.96 kPa, while its maximum equivalent stress is 498.69 kPa.

Materials and methods

CHAPTER III

MATERIALS AND METHODS

This chapter details the methods used for developing a soft robotic pineapple gripper. The entire methodology is described including the physical and mechanical properties of pineapple, design and finite element analysis of soft robotic pineapple gripper.

3.1 PHYSICAL AND MECHANICAL PROPERTIES OF PINEAPPLE

Physical properties of pineapple primarily assessed by evaluating fruit parameters such as shape, size, length and diameters at top, middle and bottom positions which were then used for the design and development of soft robotic pineapple gripper. Mechanical properties include weight and firmness of pineapple.

3.1.1 Physical properties of pineapple

The shape of the pineapple assumed to be an inverted cone with a slight tapering at the top and bottom portion as shown in Fig.3.1.

Fig.3.1 Pineapple

The top and bottom diameters of the fruit are important decision parameter that determines the dimensions of the casing of soft robotic gripper. Whereas middle diameter decides the length of single finger of soft gripper. The girth of the

pineapple at the middle portion was measured by encircling using a thread. Length of the thread was then measured by steel rule of least count 0.5 mm. Half of this measurement was taken as the length for the design of soft gripper. Measurement of diameter of pineapple using a vernier calliper. Transverse diameter of pineapple was measured by taking the diagonal measurement. This diameter helps to decide the number of grippers required for operation. The measurement was taken by using a steel rule of least count 0.5 mm.

Total length of the pineapple was measured from the bottom point of crown to the top point of the peduncle. It is essential to design the length of gripper casing. Measurement was taken using a steel rule of least count 0.5 mm.

3.1.2 Mechanical properties

The weight of pineapple is an important property that determines the gripping strength required and the type of gripper material. The weight of each sample was measured using a weighing balance of least count 0.1 kg.

Plate 1. Top, middle and bottom diameter of pineapple

Plate 2. Transverse diameter of pineapple

Firmness indicates the maximum force that can be applied on the pineapple without causing any damage. It was measured by compression test using EZ-SX texture analyzer with the operation software TRAPEZIUM X. A flat-tip cylindrical probe of 36 mm diameter was used to attain compression. The probe was placed at a distance of 10 mm from the contact surface of the sample pineapple. The speed of the prob was kept constant at 30 mm·min $^{-1}$ throughout the compression test.

Plate 3. Texture analysis of pineapple fruit

3.2 DESIGN AND DEVELOPMENT OF SOFT GRIPPER

Physical and mechanical properties of pineapple assessed by evaluating fruit parameters which were then used for the design and development of soft robotic

pineapple gripper. Among the different actuation technologies, pneumatic actuation technology was used because of its high bending angle at low pressure. Soft robotic pineapple gripper was designed by considering 5th to 95th percentile of all the measured physical and mechanical properties. Soft gripper has been developed using design/ CAD software – SolidWorks. Optimisation of gripper has been carried out by considering geometry (triangle, rectangle and half round), materials (Ecoflex-0030, Dragonskin 0030 and Smoothsil 950) at different pressures using finite element analysis of soft grippers with the help of ANSYS workbench R2.

3.2.1 Design of soft grippers

3.2.1.1 Design Considerations and Assumptions

Soft robotic pineapple gripper was designed by considering 5th to 95th percentile of all the measured physical and mechanical properties. Following are the design consideration and assumptions of this research work.

a) Length of single finger of the soft gripper was considered to be half of the 95th percentile value of the middle girth of the pineapple.

b) Number of fingers in the soft gripper was decided by considering transverse diameter of the pineapple.

c) Gripper material was selected by considering the firmness of the pineapple because harder the material, more likely to cause damage to the pineapple and softer the material, more likely to cause damage to the gripper because of the thorns in the pineapple.

d) 95th percentile value of the firmness of the pineapple was considered to decide maximum actuation pressure required to hold the pineapple.

e) Gripper material was selected by assuming that it can take a net weight of 2 kg after applying a factor of safety of 1.25.

Maximum weight of pineapple = 1.56 kg

Factor of safety = 1.25 Net weight = 1.56 × 1.25 = 1.95 kg.

3.2.1.2 Selection of Mechanism to Operate the Gripper

The robotic grippers for fresh fruits must fulfil special requirements such as maximum adherence at minimal pressure, no damage to the product, low maintenance, high reliability, low weight, be approved for contact with foodstuffs, required positional precision for both gripping and releasing of the product. All the above-mentioned factors are considered to specify gripping manipulation and to design a gripper.

Some of the direct contact type strategies for grippers include pneumatic, thermal, hydraulic, magnetic and electrical methods. Among these, a pneumatic type gripper, was selected considering simplicity and easiness in construction. The other designs are too complicated, heavy and more likely to cause damage to fruit while gripping. The gripping action can be achieved mainly by three technologies viz, gripping by actuation, gripping by controlled stiffness and gripping by controlled adhesion.

Gripping by actuation entails bending of gripper fingers/parts to encircle the object, similar to how we pick up an egg or a glass of water with our fingers. The bending shape can be actively controlled, or deformation can be induced by contacting the object. Gripping by controlled stiffness is achieved by gripping with regulated stiffness that disturbs differences in the rigidity of particular materials or material combinations. Phase change materials like Electrorheological (ER) or Magnetorheological (MR) fluids, granular jamming, low-melting-point alloys and shape memory polymers are excellent options. Whereas, controlled adhesion gripping necessitates an actuation method to wrap the item partially. Surface forces between gripper and object at the interface are used to control adherence by electro adhesion or dry adhesive (can also be called gecko adhesive). By considering the aim to pick pineapple, finger like gripping (gripping by actuation) is recommended.

3.2.1.3 Material Optimisation

The material should have a reasonable stiffness to provide enough bending angle and blocking force to perform grasping tasks for soft robotic gripper

applications. Material properties such as viscoelasticity, stiffness, and maximum elastic deformation has effect on certain factors like response time of the gripper, the force it can generate, and its stroke. Therefore, designing of grippers with improved capabilities relay on selection of material and engineering. Some of the materials like Dragonskin 30, Ecoflex-0030 and Smooth-sil-950 was selected as the construction material.

Table 3.1. Properties of materials

Properties	Ecoflex-0030	Dragonskin 0030	Smoothsil-950
Shore hardness	0030	30A	50A
Specific gravity	1.07g/cc	1.08g/cc	1.24g/cc
Tensile strength	200psi	500psi	725psi
Cure time	4 hours	16 hours	18 hours
Useful temperature (min)	-65ºF	-	-65ºF
Useful temperature(max)	450ºF	-	450ºF
Mixed viscosity	3000cps	20000cps	35000cps

3.2.1.4 Geometry Optimisation

Another important step was the selection of a suitable gripper geometry. In this study, the gripper used was a cantilever beam in which one-end fixed and other-end is free. Rectangular cross section, half-round cross section and triangular cross section were selected. Geometrical optimisation was carried out by developing 3 grippers. The parameters such as length of gripper, thickness of wall, bottom width, gap between adjacent channels, height of the model gripper were taken as 143, 2.50, 25, 1.80, 35 mm respectively with 9 number of channels as shown in Fig. 3.2.

The length of soft gripper was taken as 143 mm by considering the average middle diameter of pineapple. Results of previous studies shows that if the wall thickness was 3.00 mm, the bending change of the actuator will be very small. Even if the pressure increases to about 90 kPa, the bending amplitude of the soft gripper cannot achieve good results in the actual grasping process; thus, it was not desirable.

When the wall thickness was greater than 2 mm, the bending radius will be less than 2 mm. When the wall thickness was 2.50 mm, the bending angle will be in line with that of the expected results. Therefore wall thickness of 2.50 mm was considered.

A smaller gap between the chambers can be expected to generate a larger bending angle so that a smaller gap could be used. When 0.50 mm and 1 mm gaps are used, the adjacent channels will touch each other. However, there will not be contact between the adjacent channels when 2 mm gaps are applied. Though the interaction force between the channels can potentially generate larger bending angles, it may also cause damage to the channels. Therefore, a 1.80 mm gap is more suited in this design to prevent the bursting issue and to produce a relatively broad bending angle.

From the previous experimental results, if seven cavities are selected, the sealing of the soft gripper will be broken when the air pressure reaches 50 kPa. If 10 mm cavities are selected, the weight of the soft gripper will increase. Therefore, through comprehensive analysis and comparison, the nine-cavity soft gripper was finally used in the experiment.

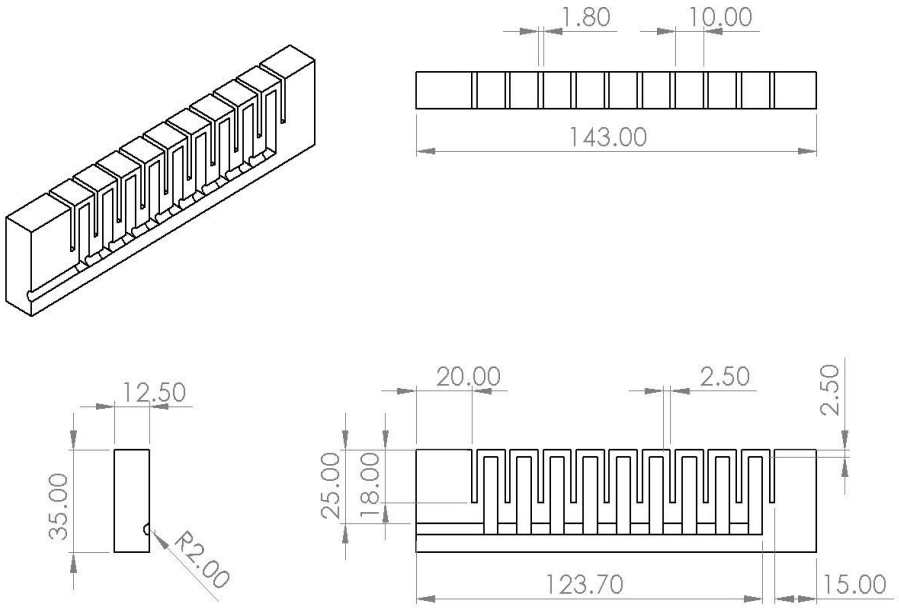

Fig.3.2 Rectangular cross section done in solidworks

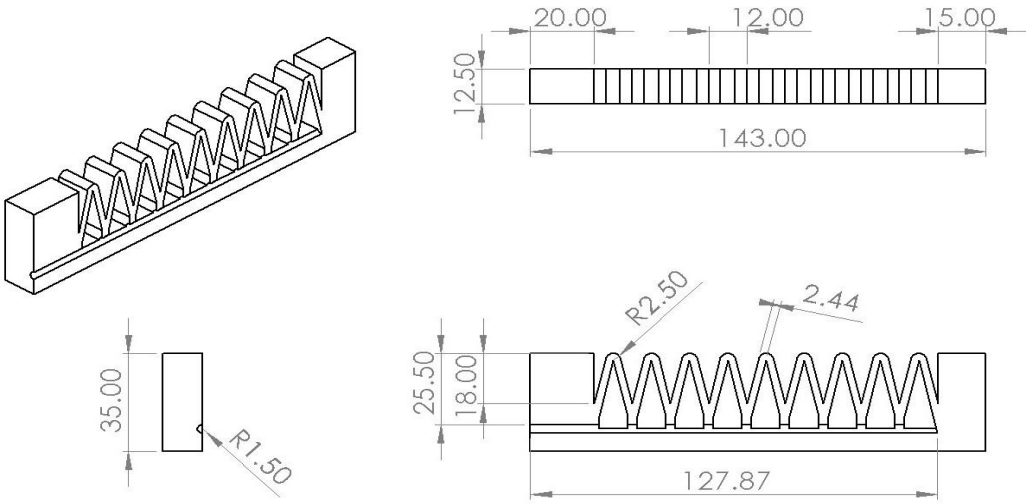

Fig.3.3 Triangular cross section done in solidworks

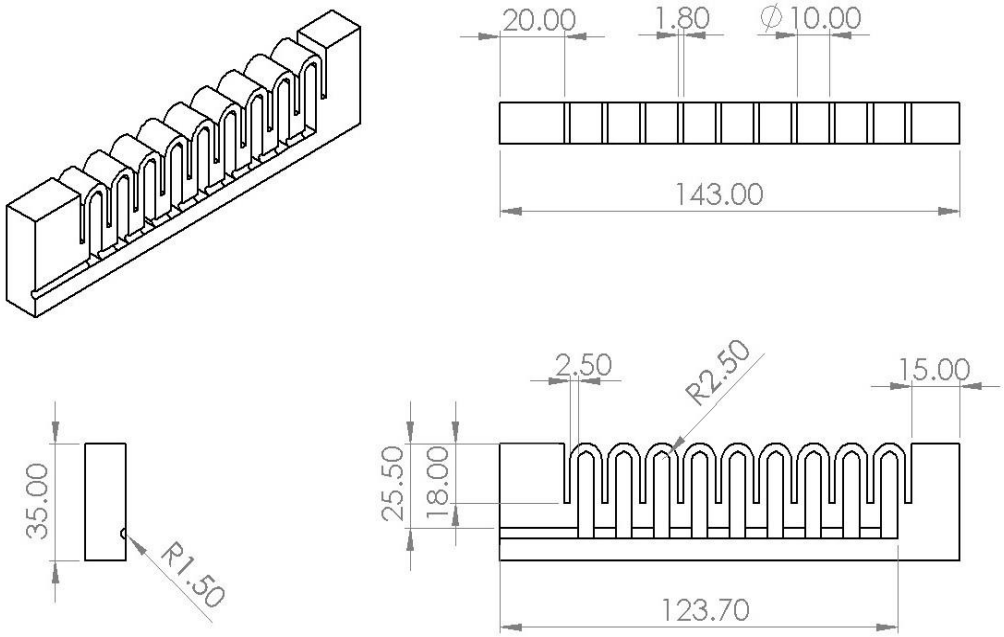

Fig.3.4 Half-round cross section done in solidworks

Finite element analysis of the designed gripper was done in ANSYS software. Large deformation effects in the finite element model were taken into account.

3.2.2 Finite Element Analysis of a Designed Gripper

In this work the finite element analysis of soft grippers was done with the help of ANSYS workbench R2 to efficiently predict their behaviour. Finite Element Method (FEM) is a numerical method, seeking an approximated solution of the distribution of field variables, such as stress and displacement, in the problem domain. It is useful in existing product refinement and new product design by demonstrating how the product responds to certain conditions such as loading, pressurising etc. This is done to ensure that most appropriate material and parameters are chosen for the development of gripper. In order to perform FEM, a model of a single gripper finger to be analysed was constructed and the resulting geometry was divided into a finite number of discrete elements (i.e. FE mesh generation), connected at discrete points called nodes. Each element contains its own material and structural properties which define how the structure will react to certain loading conditions. Together with the predefined loads and boundary conditions, the response of the model to any form of external loadings was predicted and the results were visualised in coloured contours representing different stress levels and displacements in the model. Models of soft pneumatic grippers were constructed using SolidWorks.

3.2.2.1 Simulation of Soft Finger

The parts of the soft actuator drawn by using SolidWorks software were imported into ANSYS in STEP file format. The material behaviours of elastomers used were taken from the properties given in the table (3.1) and it was used to model the element. The model was then discretized into a number of elements by meshing. A sizing function was used to get a mesh with a specific element size of 1.0 mm. In the analysis settings ‘large deflection’ option was activated as the soft gripper exhibits large deformations on application of working pressure. Also substeps were introduced to gradually apply the load. One end of the gripper with a solid chamber

was kept fixed and standard earth gravity was applied for the analysis. Then different actuation positive pressures were applied at all internal surfaces of pneumatic gripper. The Ecoflex -0030 being low stiffness material, the applied pressure was also low and the pressure ranges was selected according to the failure of simulation for each geometry. Smoothsill-950 and Dragon skin -0030 having comparatively high and medium stiffness, therefore the pressure range used was more wider. The model was solved for total deformation and equivalent stress in the applied pressure ranges.

Results and discussion

CHAPTER IV

RESULTS AND DISCUSSION

The physical and mechanical properties of pineapple, development of soft robotic pineapple gripper and performance evaluation of soft robotic pineapple gripper are explained in detail and the results are discussed in this chapter.

4.1 PHYSICAL PROPERTIES AND MECHANICAL PROPERTIES OF PINEAPPLE

Physical properties include shape and size of pineapple, vertical length, diameters at top, middle, bottom positions of the pineapple were studied. Mechanical properties such as weight and firmness of pineapple were discussed. The result thus obtained is shown in the Table 4.1

4.1.1 Physical properties of pineapple

Pineapple have cylinder like shape with slight tapering both at top and bottom. An average tapering angle of about 12º was found at the top and 8º was found at the bottom after taking the measurement. From the Table 4.1, it is observed that, it has minimum top diameter of 6.30 cm and maximum top diameter of 9.50 cm. Average value of top diameter was found to be 7.74 cm. Middle diameter of pineapple has a minimum value of 9.30 cm and maximum of 11.50 cm. This portion of pineapple was found to have more diameter as compared to top and bottom. 10.14 cm was the average value of middle diameter. The average bottom diameter was 9.53 cm. Maximum value of bottom diameter was 11.50 cm and minimum value was 8.40 cm. Pineapple has a maximum transverse diameter of 19.50 cm. Minimum and average transverse diameters were 11.50 cm and 16.35 cm respectively. Pineapple has an average vertical length of 19.32 cm. Maximum vertical length was 23 cm whereas minimum was 15.50 cm.

4.2 MECHANICAL PROPERTIES OF PINEAPPLE

Maximum weight of pineapple was measured to be 1.56 kg. Minimum weight of the pineapple was 1.11 kg and average weight was found to be 1.36 kg. The firmness of pineapple was obtained from the texture analyser data of compression test. Compression test was done at two positions, top and bottom of each pineapple. The average firmness of the pineapple at a cutting speed of 30 $mm.min^{-1}$ was obtained as 3.75 $N.cm^{-2}$.

Table 4.1 Physical and mechanical properties of pineapple

Sl. No.	Weight (kg)	Vertical length (cm)	Top diameter (cm)	Middle diameter (cm)	Bottom diameter (cm)	Transverse diameter (cm)
1	1.56	21.00	6.90	9.60	9.40	18.00
2	1.44	20.50	7.80	9.70	9.30	17.50
3	1.25	18.00	7.20	9.30	9.10	16.00
4	1.55	21.00	6.90	9.40	9.00	18.50
5	1.42	23.00	6.30	9.45	8.40	19.50
6	1.45	20.50	7.60	10.10	9.20	17.00
7	1.52	22.50	7.60	9.50	9.40	19.50
8	1.40	20.00	7.40	9.70	9.50	17.00
9	1.28	18.00	7.70	9.80	9.40	15.50
10	1.26	17.00	8.00	11.00	11.50	14.00
11	1.31	21.00	8.00	10.00	9.80	18.00
12	1.23	16.50	8.50	11.50	10	13.50
13	1.11	16.00	9.50	12.00	10	13.50
14	1.30	15.50	9.00	11.00	9.50	11.50

4.3 DESIGN OF GRIPPER

The finger of the soft gripper was designed in such a way that it should have maximum adherence at minimal pressure, cause no damage to the product, low maintenance, high reliability, low weight, be approved for contact with foodstuffs, requires positional precision for both gripping and releasing of the product. Out of different contact strategies, pneumatic type gripper was selected. Selection was based on the construction easiness as the other designs were too complicated, heavy and more likely to cause damage to fruit while gripping. Among the gripping technologies, gripping by actuation was selected, preferably pneumatic actuation. Because it can achieve finger like gripping.

4.4 FINITE ELEMENT ANALYSIS OF A DESIGNED GRIPPER

Finite element analysis was carried out to understand the behaviour of a material under different physical conditions. The design of the gripper was made using SolidWorks. The parts of the soft actuator were imported into Ansys in STEP file format.

4.4.1 Ecoflex-0030

4.4.1.1 Ecoflex-0030 with half round geometry

Mesh sorting allowed the model to become discretized into several elements. To obtain a mesh with a specified element size of 2 mm, a sizing function was employed. The number of elements and nodes obtained are 11937 and 3799 respectively. The "large deflection" option in the analysis settings was activated because the soft gripper shows significant deformations when working pressure is applied. The load was applied progressively by adding substeps. For the analysis, the gripper's solid chamber end was fixed, and standard earth gravity was used. Positive pressures were then applied to all internal surfaces of the pneumatic channels for actuation.

To optimize the material and geometry, simulations were run at various pressures 5, 8, 10 and 10.5 kPa. Corresponding bending angle and equivalent stress

in different pressure range is shown in fig. 4.1 and fig. 4.2 respectively. Results of parameterisation is shown in Table 4.2.

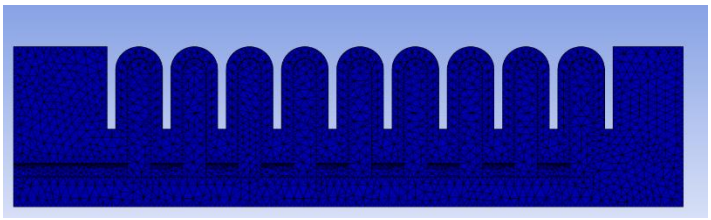

(a)

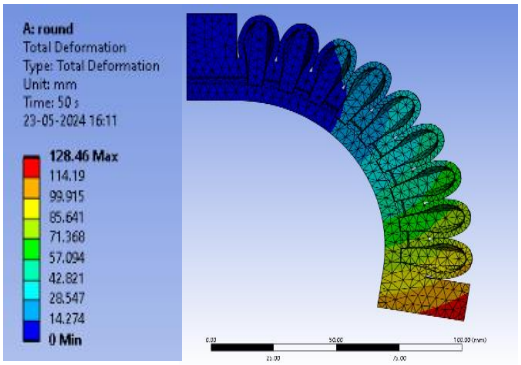

(b)

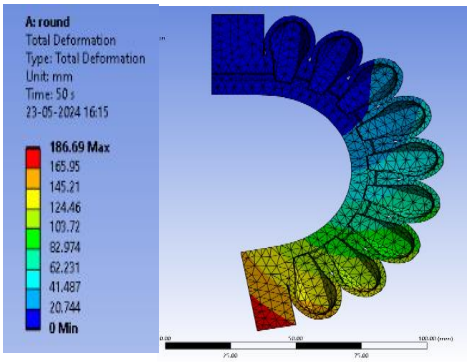

(c)

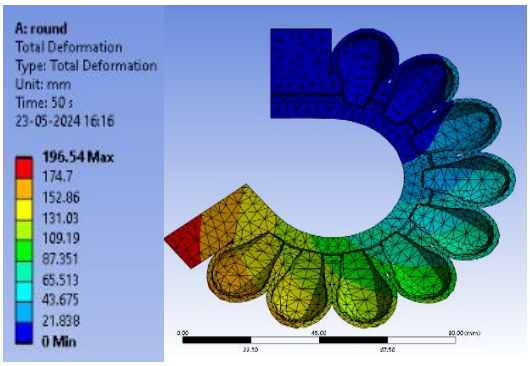

(d)

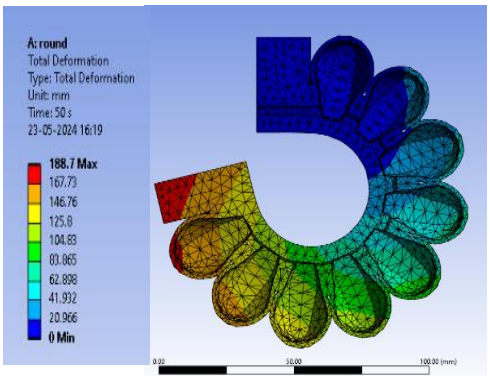

(e)

Fig.4.1 Total deformation at different pressures in Ecoflex-0030 with half round geometry.(a)At No pressure (b) At 5 kPa, (c) At 8 kPa, (d) At 10 kPa, (e) At 10.5 kPa

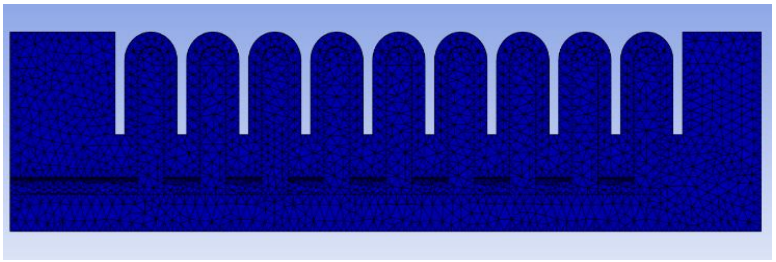

(a)

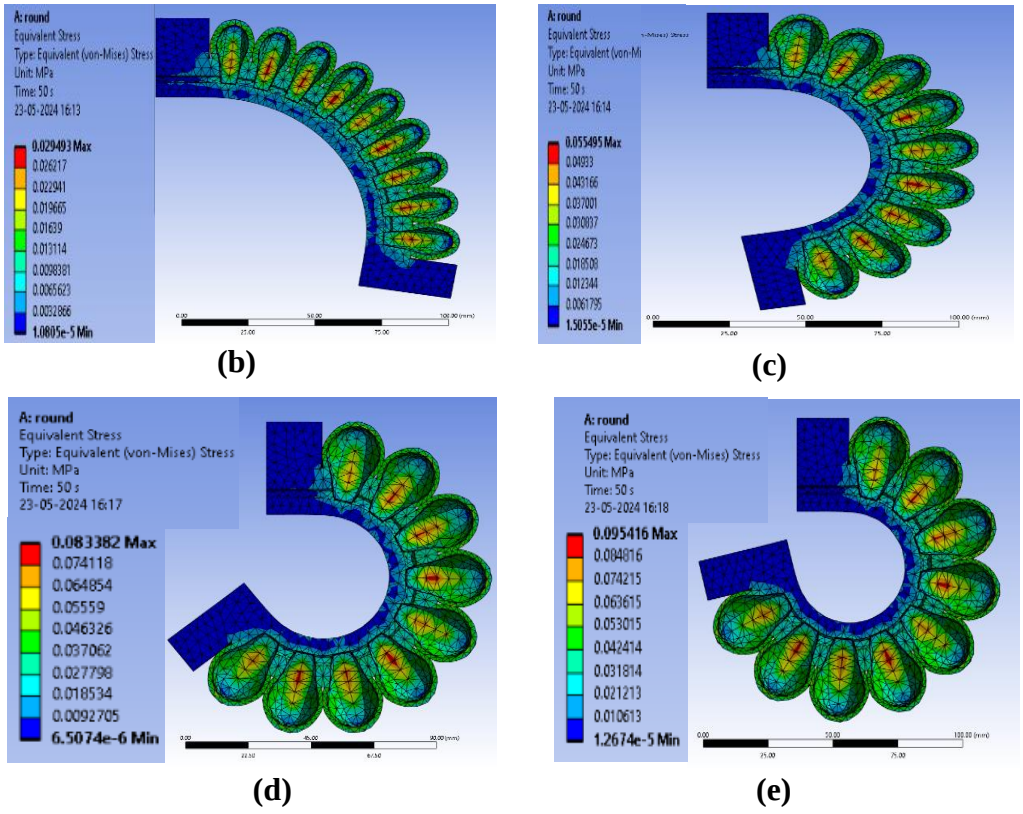

Fig.4.2 Equivalent stress at different pressures in Ecoflex-0030 with half round geometry. (a) At No pressure (b) At 5 kPa, (c) At 8 kPa, (d) At 10 kPa, (e) At 10.5 kPa

Table 4.2 parameterisation of Ecoflex-0030 with half round geometry

Sl. No.	Pressure (kPa)	Bending Angle (degree)	Equivalent Stress Maximum (kPa)
1	5	99º	29.49
2	8	169º	55.50
3	10	232º	83.38
4	10.50	257º	95.42

From the fig.4.1, it is observed that for Ecoflex-0030 with half round geometry, the applied pressures 5, 8, 10 and 10.5 kPa give bending angles 99, 169, 232 and 257 degrees respectively. Above the pressure 10.5 kPa, the simulation was

a failure, which may due to the breakage of gripper. Fig. 4.2 illustrates the equivalent stresses, which is from 29.49 to 95.43 kPa.

As pressure increases, the circular chamber inflates uniformly, causing the gripper finger to bend outwards in a more radial fashion. This creates a conforming grip around objects of varying shapes. The symmetrical nature of the circular chamber promotes a more uniform distribution of stress compared to rectangular chambers. This can be beneficial for reducing the risk of localized stress concentrations that might lead to failure. Circular chambers might achieve a slightly lower maximum bending angle compared to rectangular chambers under the same pressure due to the more uniform inflation pattern. As air expands inside the chamber, it pushes outwards with relatively equal force in all directions around the circumference. This inflation pattern results in a more gradual outward bending of the gripper finger.

4.4.1.2 Ecoflex-0030 with rectangle geometry

The model was discretized into a number of elements by meshing. A sizing function was used to get a mesh with a specific element size of 1 mm. The number of elements and nodes obtained are 45952 and 12924 respectively. To optimize the material and geometry, simulations were run at various pressures 5, 8, 9 and 10 kPa. Corresponding bending angle and equivalent stress in different pressure range is shown in fig. 4.3 and fig. 4.4 respectively. Results of parameterisation is shown in Table 4.3.

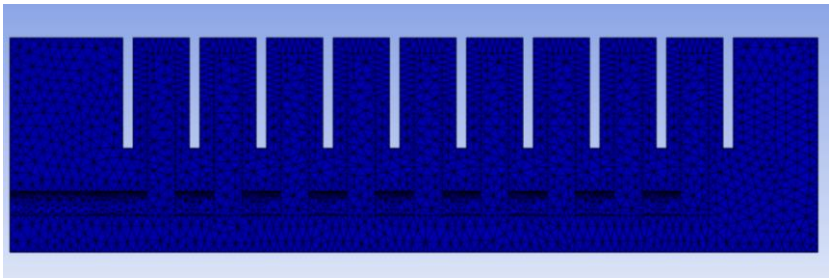

(a)

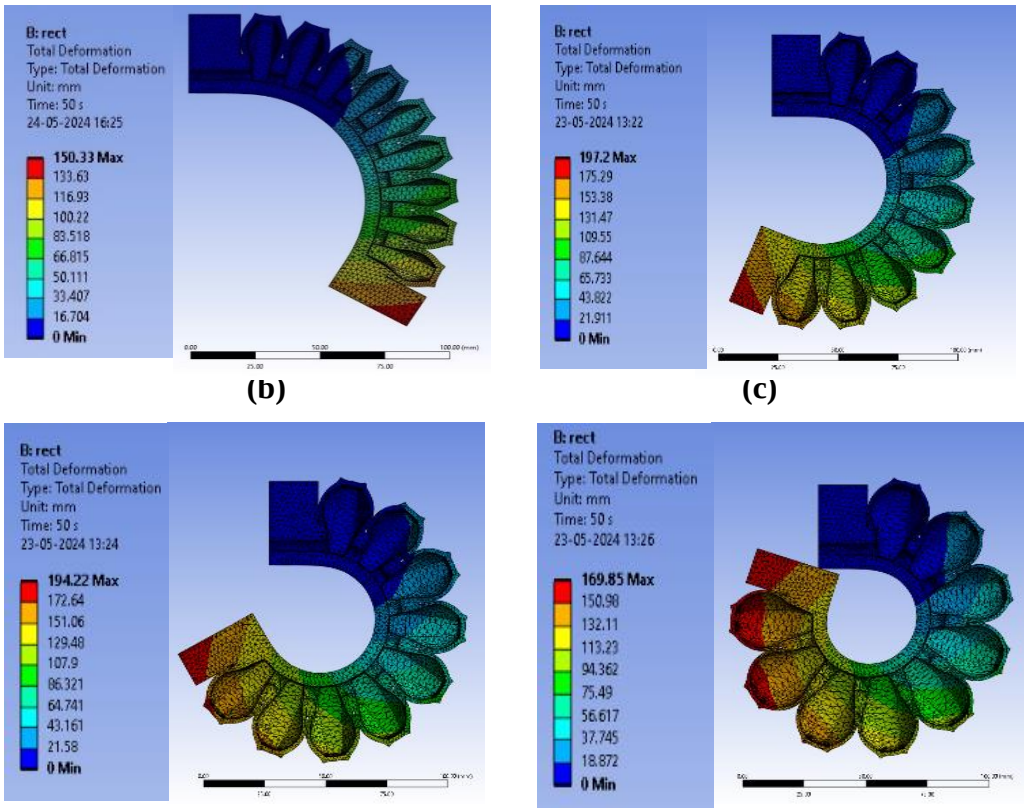

(b) **(c)**

(d) **(e)**

Fig.4.3 Total deformation at different pressures in Ecoflex-0030 with rectangle geometry. (a)At No pressure (b) At 5 kPa, (b) At 8 kPa, (c) At 9 kPa, (d) At 10 kPa

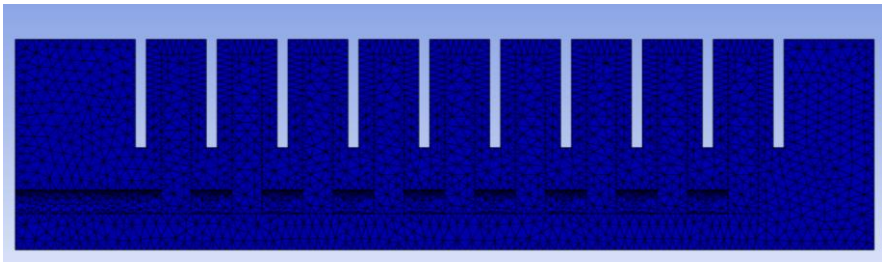

(a)

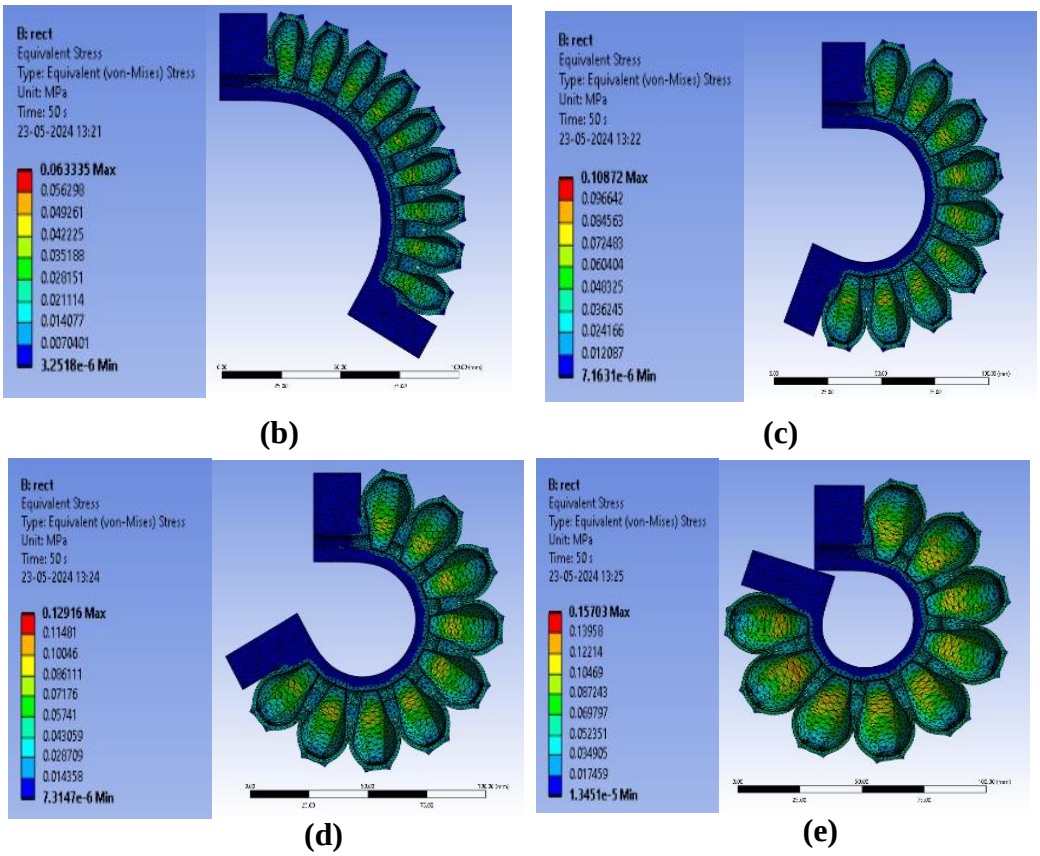

Fig.4.4 Equivalent stress at different pressures in Ecoflex-0030 with rectangle geometry.(a) At No pressure (b) At 5 kPa, (c) At 8 kPa, (d) At 9 kPa, (e) At 10 kPa

Table 4.3 parameterisation of Ecoflex-0030 with rectangle geometry

Sl. No.	Pressure (kPa)	Bending Angle (degree)	Equivalent Stress Maximum (kPa)
1	5	120º	63.33
2	8	201º	108.72
3	9	240.8º	129.16
4	10	289º	157.03

From the fig.4.3, it is observed that for Ecoflex-0030 with rectangle geometry, the applied pressures 5, 8, 9 and 10 kPa gives bending angle of 120, 201, 240.8 and 289 degrees respectively. Above the pressure 10 kPa, the simulation was

a failure, which may due to the breakage of gripper. Fig. 4.4 illustrates the equivalent stresses, which is from 63.33 to 157.03 kPa.

Inflation in a rectangular chamber primarily occurs in two directions – perpendicular to the longer sides. This creates a more focused inflation pattern, where the air pressure exerts a greater force on the shorter sides compared to the longer sides. This focused inflation concentrates the bending effect on the shorter sides, causing them to bulge outwards more prominently.

4.4.1.3 Ecoflex-0030 with triangle geometry

The number of elements and nodes obtained are 42718 and 12042 respectively. To optimize the material and geometry, simulations were run at various pressures 6, 7, 8 and 9 kPa. Corresponding bending angle and equivalent stress in different pressure range is shown in fig. 4.5 and fig. 4.6 respectively. Results of parameterisation is shown in Table 4.4.

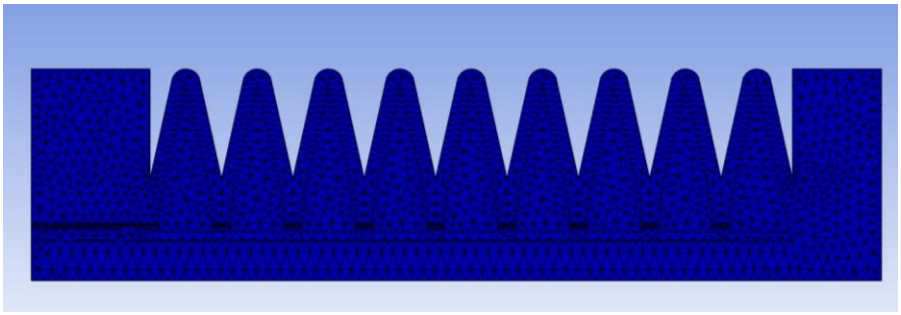

(a)

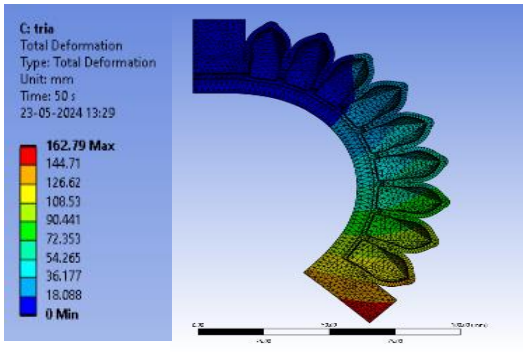

(b)

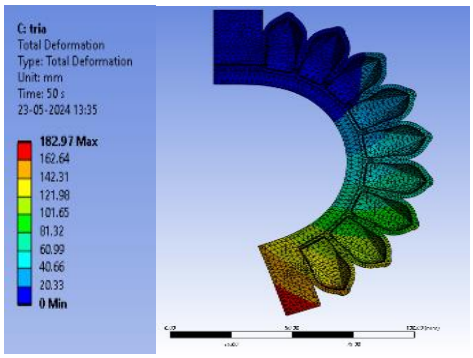

(c)

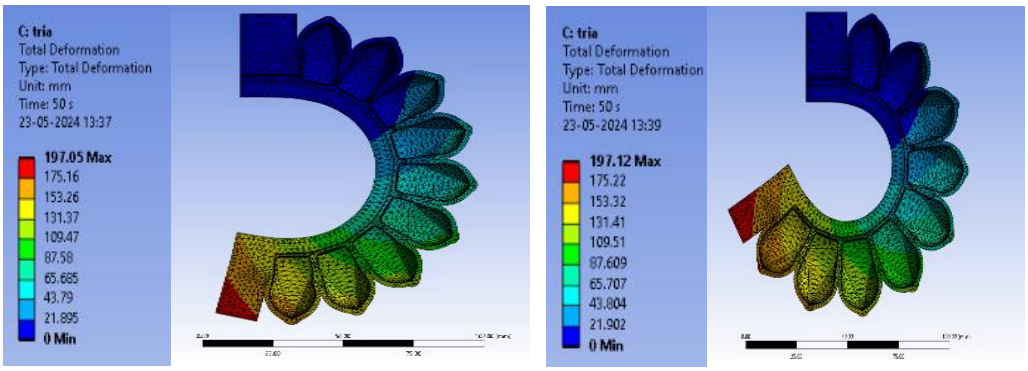

(d) **(e)**

Fig.4.5 Total deformation at different pressures in Ecoflex-0030 with triangle geometry. (a) At No pressure (b) At 6 kPa, (c) At 7 kPa, (d) At 8 kPa, (e) At 9 kPa

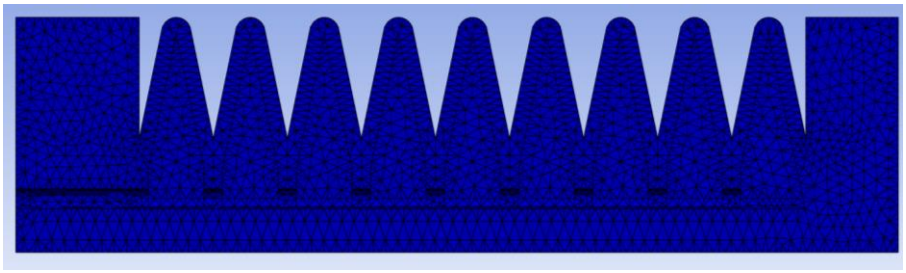

(a)

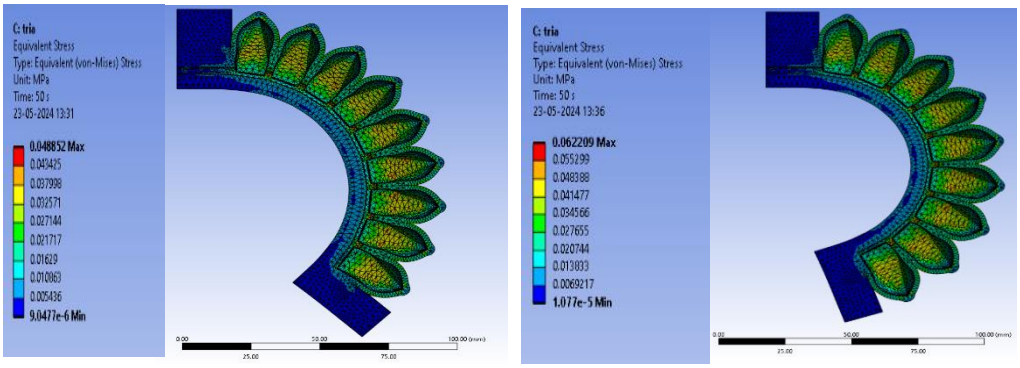

(b) **(c)**

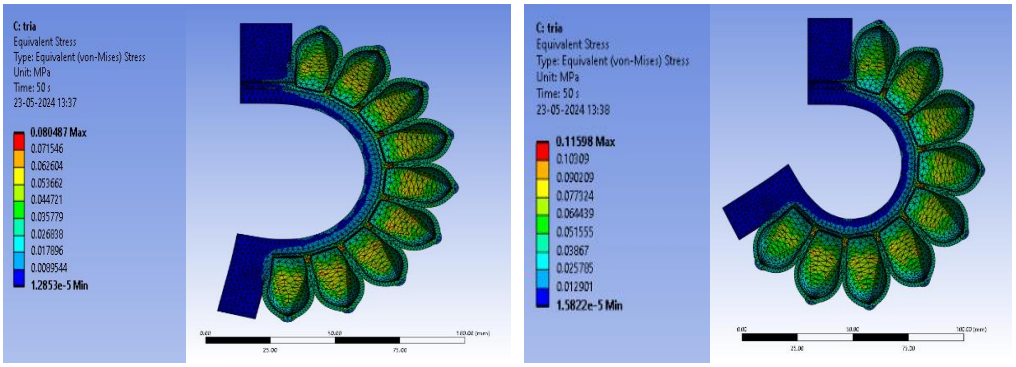

(d) **(e)**

Fig.4.6 Equivalent stress at different pressures in Ecoflex-0030 with triangle geometry. (a) At No pressure (b) At 6 kPa, (c) At 7 kPa, (d) At 8 kPa, (e) At 9 kPa

Table 4.4 parameterisation of Ecoflex-0030 with triangle geometry

Sl. No.	Pressure (kPa)	Bending Angle (degree)	Equivalent Stress Maximum (kPa)
1	6	134º	48.85
2	7	161º	62.21
3	8	193º	80.49
4	9	239º	115.98

From the fig.4.5, it is observed that for Ecoflex-0030 with triangle geometry, the applied pressures 6, 7, 8 and 9 kPa gives bending angle of 134, 161, 193 and 239 degrees respectively. Fig. 4.6 illustrates the equivalent stresses, which is from 48.85 to 115.98 kPa.

Out of the three available geometries, the half-round geometry has the lowest stress range and can handle higher pressures for this particular material. Rectangle geometry was the one which show maximum bending angle of 289 degree and maximum stress of 155.70 MPa. Triangle geometry have a moderate

angle and stress range in contrast to other shapes, however its simulation failed at an earlier pressure than other shapes.

As the stiffness of the material decreases elongation increases, which is the reason why ecoflex 30 gives higher bending angle in low pressure. The bending direction in triangular chambers depends on the orientation of the apex (pointed end). With the apex outwards, inflation causes bending towards the base, creating a scooping or pinching motion. Conversely, with the base outwards, bending occurs outwards from the apex. Triangular chambers can introduce complex stress patterns depending on the specific design and inflation pattern. Careful design and analysis are crucial to ensure the material can handle the stress distribution.

4.4.2 Smooth sil-950

4.4.2.1 Smooth sil-950 with half round geometry

The model was discretized into a number of elements by meshing. A sizing function was used to get a mesh with a specific element size of 1 mm. The number of elements and nodes obtained are 48901 and 13867 respectively. In the analysis settings ‘large deflection’ option was activated as the soft gripper exhibits large deformations on application of working pressure. Also, sub-steps were introduced to gradually apply the load. One end of the gripper with a solid chamber was kept fixed and standard earth gravity was applied for the analysis. Then actuation positive pressures were applied at all internal surfaces of pneumatic channels.

For optimisation, half-round geometry and the material smoothsil-950 were used in the simulation. 50 kPa, 60 kPa, 70 kPa, 80 kPa, and 90 kPa of pressure were applied. Corresponding bending angle and equivalent stress in different pressure range is shown in fig. 4.7 and fig. 4.8 respectively. Results of parameterisation is shown in Table 4.5.

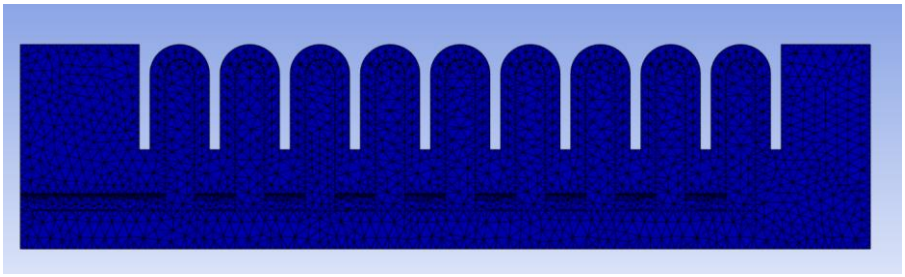

(a)

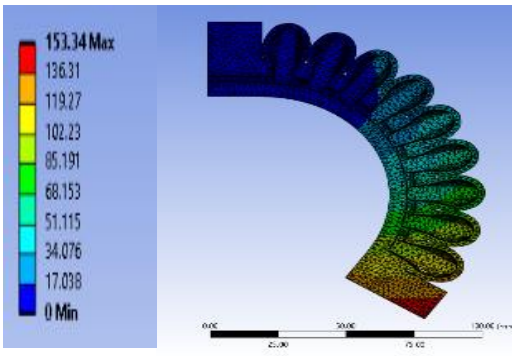

(b)

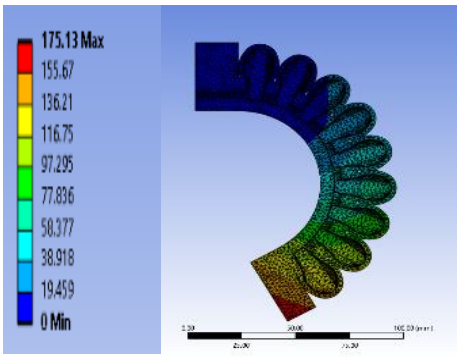

(c)

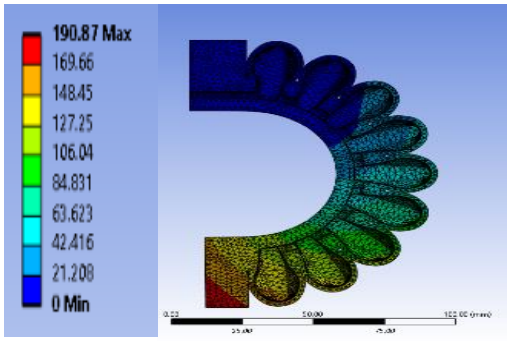

(d)

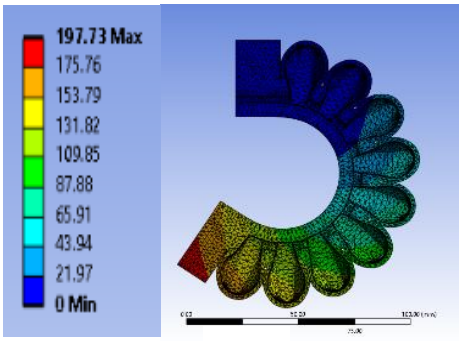

(e)

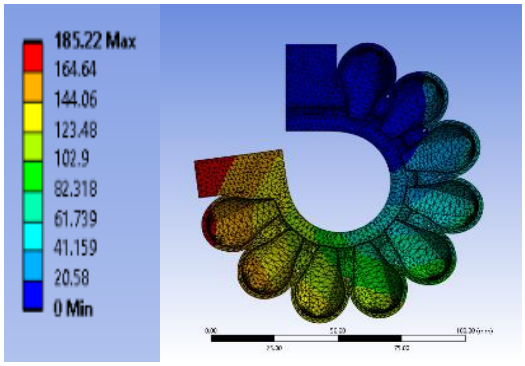

(f)

Fig.4.7. Total deformation at different pressures in Smooth sil-950 with half round geometry. (a) At No pressure (b) At 50 kPa, (c) At 60 kPa, (d) At 70 kPa, (e) At 80 kPa, (f) At 90 kPa

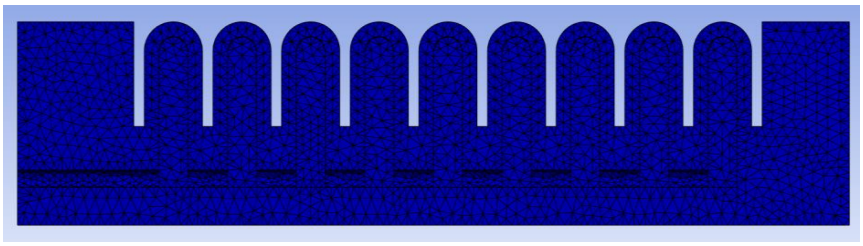

(a)

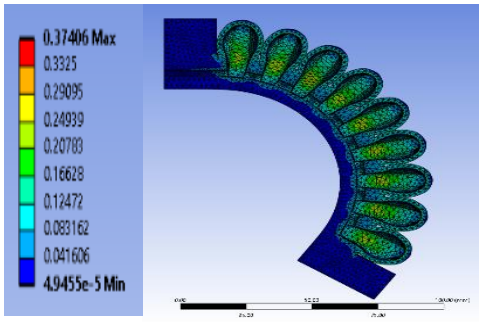

(b)

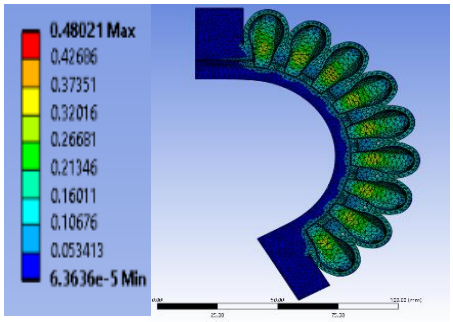

(c)

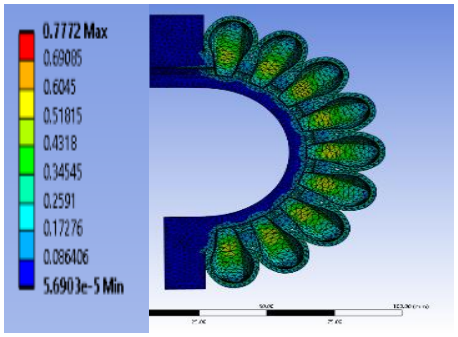

(d)

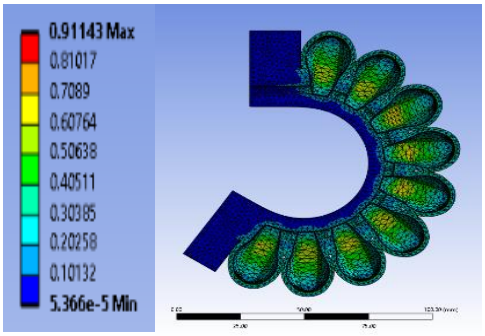

(e)

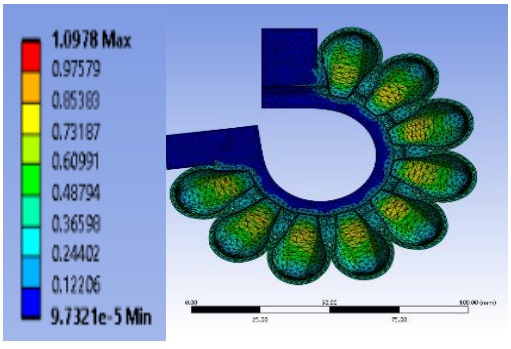

(f)

Fig.4.8. Equivalent stress at different pressures in Smooth sil-950 with half round geometry. (a) At No pressure (b) At 50 kPa, (c) At 60 kPa, (d) At 70 kPa, (e) At 80 kPa, (f) At 90 kPa.

Table 4.5 parameterisation of smoothsil-950 with half round geometry

Sl. No.	Pressure (kPa)	Bending Angle (degree)	Equivalent Stress Maximum (kPa)
1	50	125º	545.71
2	60	151º	658.80
3	70	178.5º	777.20
4	80	214º	911.43
5	90	262º	1097.80

From the fig. 4.7 it is observed that the bending angle of 125, 151, 178.50, 214 and 262 degrees were achieved for the corresponding pressure ranges. And the fig. 4.8 illustrates the equivalent stress of 545.75, 658.8, 777.20, 911.43 and 1097.80 kPa for different pressure ranges.

The pressure acts uniformly across the entire surface area of the half-round gripper in contact with the pressure source. However, the curved geometry leads to a non-uniform distribution of stress within the material. When pressure is applied, it acts on the entire contact area of the gripper's curved surface. This pressure creates a force pushing inwards. Due to the curvature, the inner (concave) surface experiences compressive stress as the material tries to compress. Conversely, the outer (convex) surface experiences tensile stress as the material stretches. The gripper resists bending due to the stiffness of the Smoothsil-950 material. However, as the pressure and resulting internal stress increase, the bending moment eventually overcomes the material's stiffness, causing the gripper to bend.

4.4.2.2 Smooth sil-950 with rectangle geometry

The number of elements and nodes used are 44952 and 12710 respectively. For optimisation, rectangle geometry and the material smoothsil-950 were used in the simulation. 50 kPa, 60 kPa, 70 kPa, 80 kPa and 90 kPa of pressure were applied. Corresponding bending angle and equivalent stress in different pressure range is

shown in fig. 4.9 and fig. 4.10 respectively. Results of parameterisation is shown in Table 4.6.

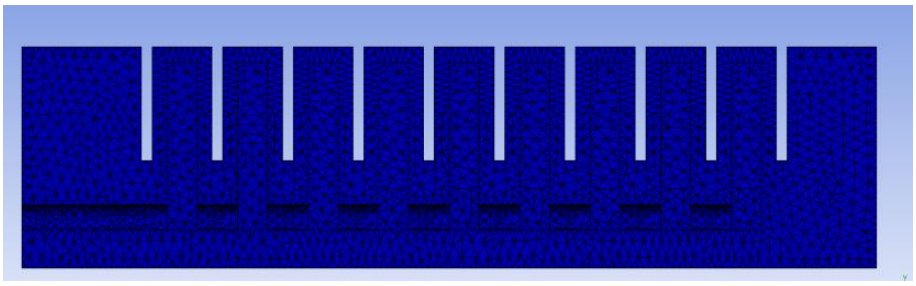

(a)

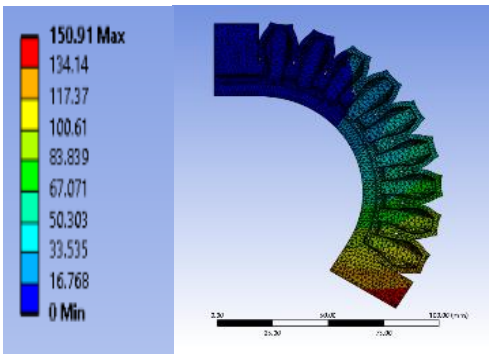

(b)

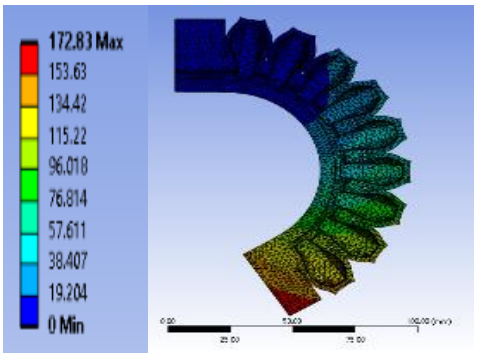

(c)

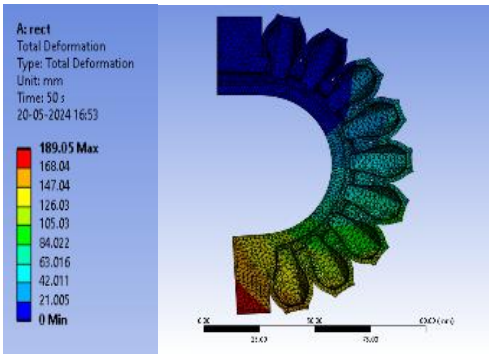

(d)

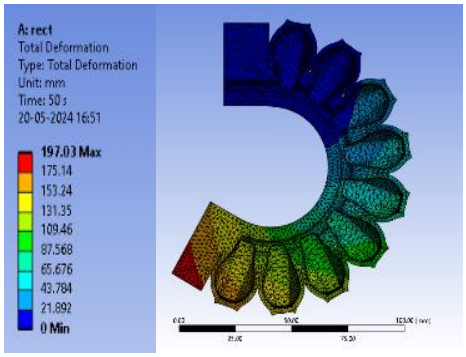

(e)

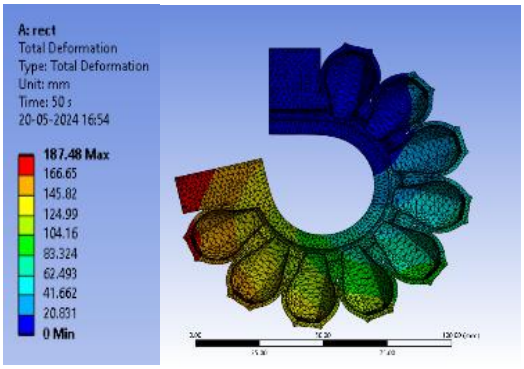

(f)

Fig.4.9. Total deformation at different pressures in Smooth sil-950 with rectangle geometry. (a) At No Pressure (b) At 50 kPa, (c) At 60 kPa, (d) At 70 kPa, (e) At 80 kPa, (f) At 90 kPa.

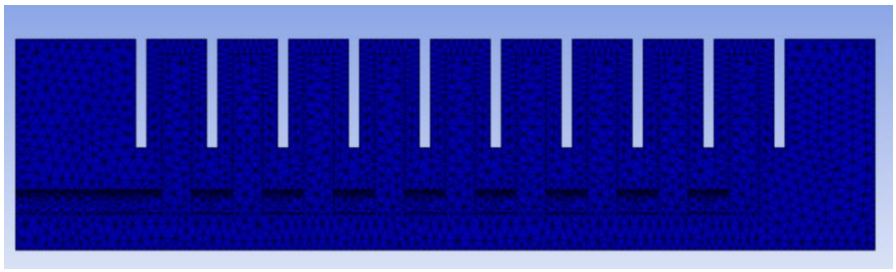

(a)

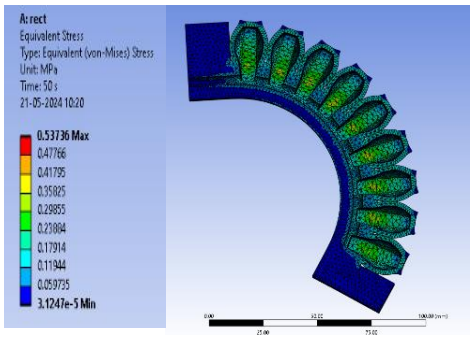

(b)

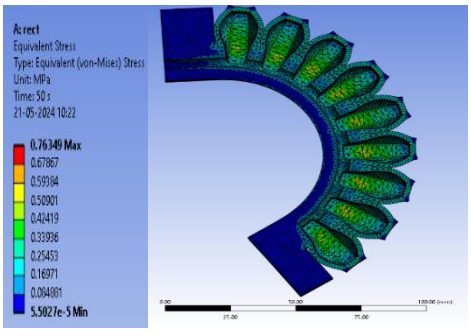

(c)

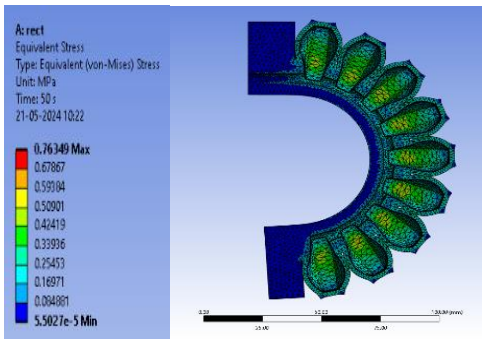

(d)

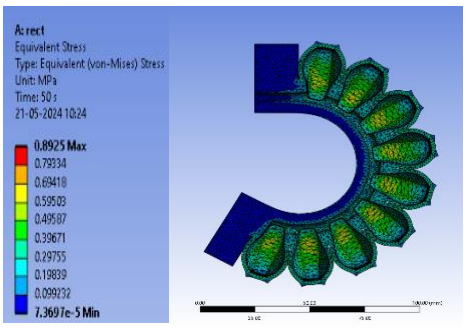

(e)

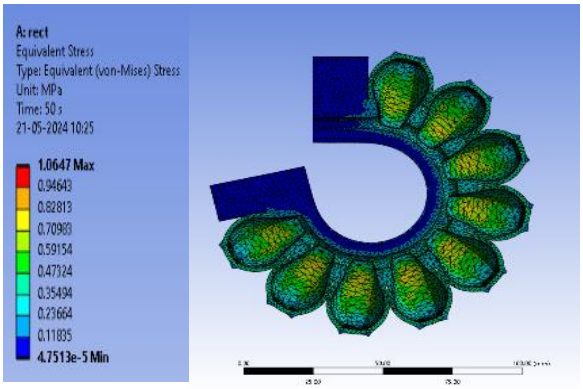

(f)

Fig.4.10. Equivalent stress at different pressures in Smoothsil-950 with rectangle geometry. (a) At No pressure, (b) At 50 kPa, (c) At 60 kPa, (d) At 70 kPa, (e) At 80 kPa, (f) At 90 kPa.

Table 4.6 parameterisation of smoothsil-950 with rectangle geometry

Sl. No.	Pressure (kPa)	Bending Angle (degree)	Equivalent Stress Maximum (kPa)
1	50	123º	537.36
2	60	148º	647.37
3	70	175.5º	763.49
4	80	209º	892.50
5	90	257º	1064.70

From the fig. 4.9 it is observed that the bending angle of 123, 148, 175.50, 209 and 257 degrees were achieved for the corresponding pressure ranges. And the fig. 4.10 illustrates the equivalent stresses for different pressure ranges, which is 537.36, 647.37, 763.49, 892.50 and 1064.70 kPa.

For the rectangular Smoothsil-950 gripper, pressure acts uniformly across the entire contact area of the rectangle where it touches the pressure source causing it to bend inwards. However, the rectangular shape leads to a stress distribution that's concentrated at the bottom edge, where the bending is most prominent. This

bending increases with higher pressure, and the bottom edge experiences the most stress due to stretching and compression. The rectangular shape makes it more prone to bending compared to the half-round geometry under similar pressures. While both geometries experience a rise in stress and bending angle with increasing pressure, the rectangular design might not be suitable for applications requiring minimal bending under high pressure due to its inherent shape and stress concentration at the bending edge.

4.4.2.3 Smooth sil-950 with triangle geometry

The number of elements and nodes obtained are 42718 and 12042 respectively. For optimisation, triangle geometry and the material smoothsil-950 were used in the simulation. 50 kPa, 60 kPa, 70 kPa, 80 kPa and 85 kPa of pressure were applied.

For convenience of comparison, the same pressures, except maximum being 85 kPa instead of 90 kPa was applied to the triangular geometry. Corresponding bending angle and equivalent stress in different pressure range is shown in fig. 4.11 and fig. 4.12 respectively. Results of parameterisation is shown in Table 4.7.

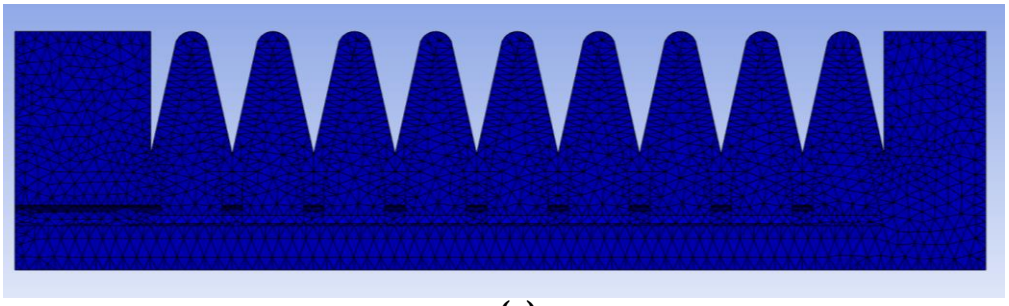

(a)

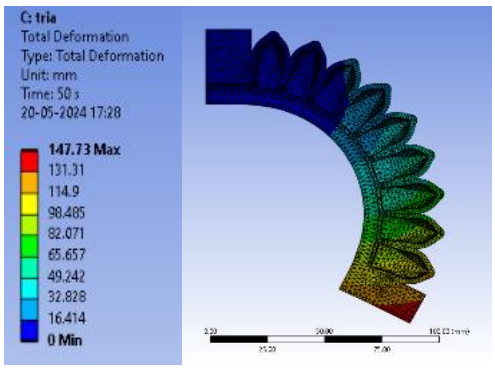

(b)

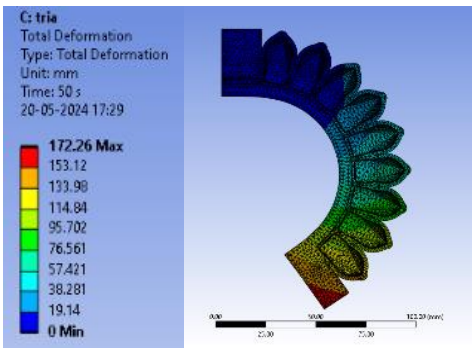

(c)

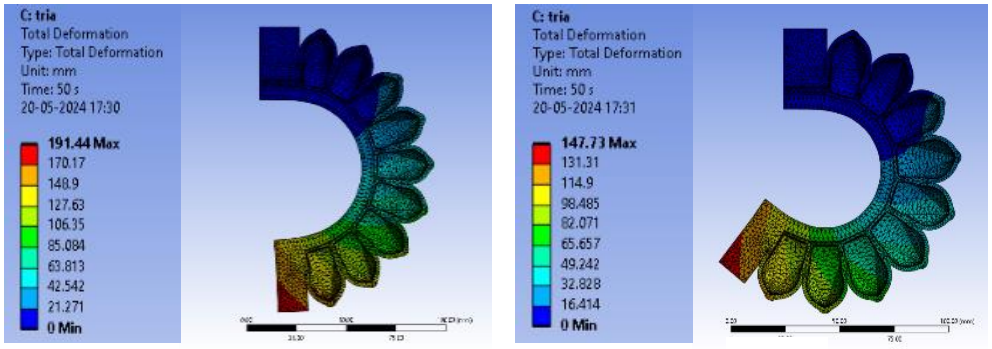

(d) **(e)**

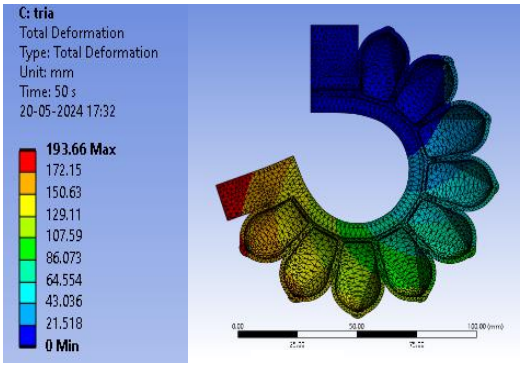

(f)

Fig.4.11. Total deformation at different pressures in Smoothil-950 with triangle geometry. (a) At No Pressure (b) At 50 kPa, (c) At 60 kPa, (d) At 70 kPa, (e) At 80 kPa, (f) At 85 kPa.

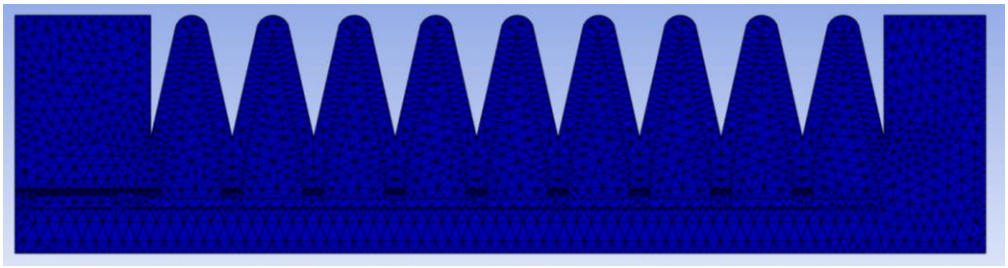

(a)

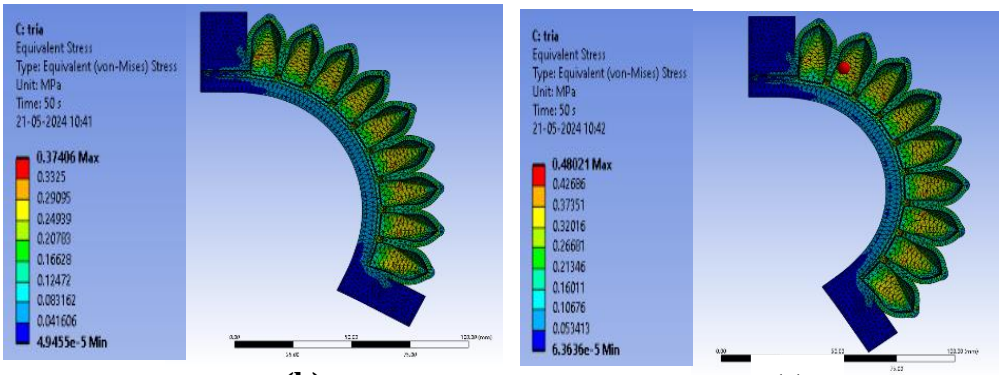

(b) **(c)**

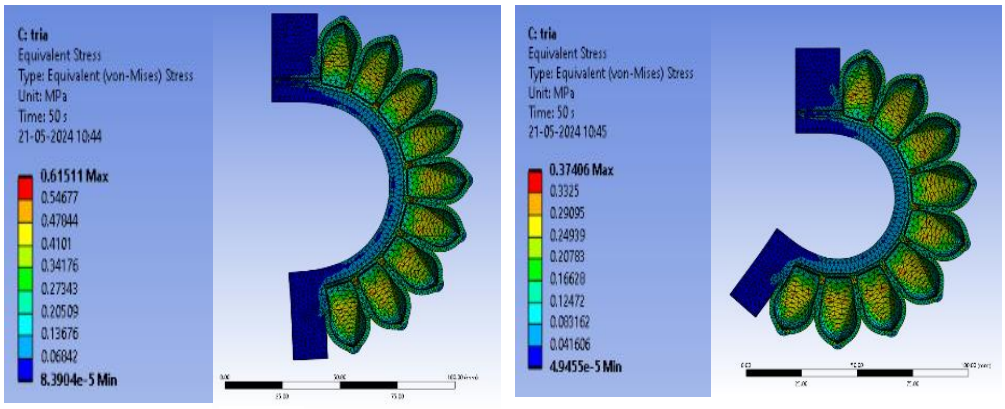

(d) **(e)**

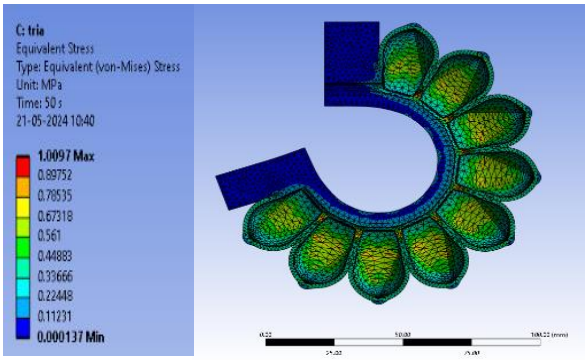

(f)

Fig.4.12. Equivalent stress at different pressures in Smoothsil-950 with triangle geometry. (a) At No pressure (b) At 50 kPa, (c) At 60 kPa, (d) At 70 kPa, (e) At 80 kPa, (f) At 85 kPa

Table 4.7 parameterisation of smoothsil-950 with triangle geometry

Sl. No.	Pressure (kPa)	Bending Angle (degree)	Equivalent Stress Maximum (kPa)
1	50	116º	374.06
2	60	145º	480.21
3	70	176º	615.11
4	80	217.5º	374.06
5	85	250º	1009.70

From the fig. 4.11, it is observed that the bending angles varying for each pressure are 116, 145, 176, 217.50, and 250 degrees. And from the fig. 4.12 it is

found that the equivalent stress for different pressure ranges are 374.06, 480.21, 615.11, 374.06, and 1009.70 kPa.

Smoothsil-950 has higher stiffness than the other two materials, which is the reason why it gives higher bending angle in higher pressure. This is because stiffer materials offer greater resistance to deformation. With the same amount of air pressure pushing outwards, a stiffer material will bend less compared to a softer material. It will distribute stress less readily. This can lead to higher stress concentrations in localized areas, potentially increasing the risk of material failure.

For smoothsil half round geometry showed comparatively higher bending angles than rectangle and triangle geometry with almost similar stress and bending angle values that obtained for rectangle geometry. Whereas for the triangle geometry there was an observable stress difference initially, which was lower than others but increased with increase in pressure, and also shown a sudden drop and rise which may be due to its special geometry, which contributes minimum contact area in expansion and also which may redirect the pressure to the base of triangle.

In comparison to rectangle and triangle geometry, half-round geometry for the smoothsil-950 showed relatively higher bending angles, with stress and bending angle values obtained for rectangle geometry being nearly same. There was an initial discernible stress differential, one that was less than the other but that increased as the pressure increased. It also displayed an abrupt rise and fall, which may have been caused by its unique geometry, which contributes to a minimum contact area and may also direct the pressure to the triangle's base.

The pressure effects on a triangular Smoothsil-950 gripper are more complex compared to rectangular or half-round geometries. Bending depends on the triangle's orientation. If the base is against the pressure, both corners might bend inwards. If the tip faces the pressure, bending might occur at the opposite corners. Regardless of orientation, stress concentrates at the bending corners. The triangle's specific angle and pressure distribution further influence how it bends and distributes stress under pressure. FEA simulations can be useful for analysing these complexities in triangular grippers.

4.4.3. Dragon skin-0030

4.4.3.1 Dragon skin-0030 with half round geometry

The model was discretized into a number of elements by meshing. A sizing function was used to get a mesh with a specific element size of 1 mm. The number of elements and nodes obtained are 48901 and 13867 respectively. In the analysis settings ‘large deflection’ option was activated as the soft gripper exhibits large deformations on application of working pressure. Also, sub-steps were introduced to gradually apply the load. One end of the gripper with a solid chamber was kept fixed and standard earth gravity was applied for the analysis. Then actuation positive pressures were applied at all internal surfaces of pneumatic channels.

For optimisation, half round geometry and the material dragonskin-0030 were used in the simulation. 30 kPa, 40 kPa, 50 kPa, 60 kPa and 70 kPa of pressure were applied. Corresponding bending angle and equivalent stress in different pressure range is shown in fig. 4.13 and fig. 4.14 respectively. Results of parameterisation is shown in Table 4.8.

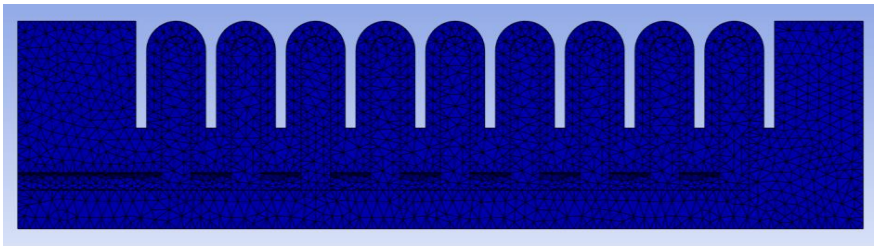

(a)

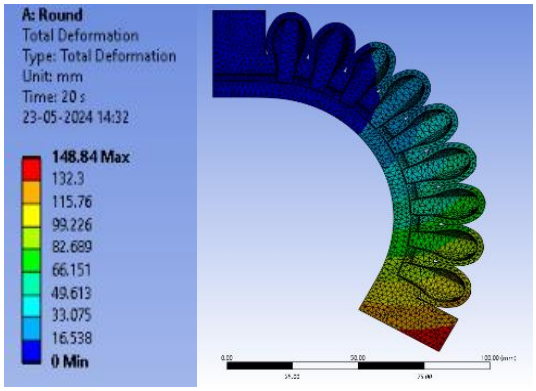

(b)

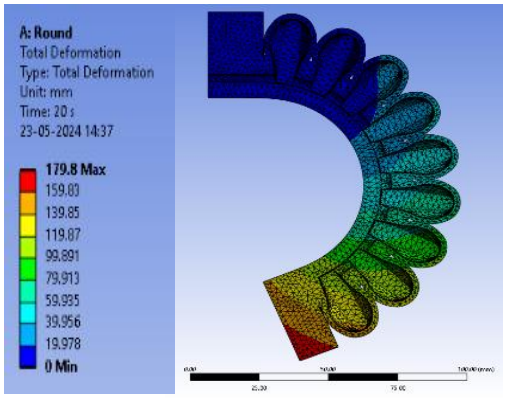

(c)

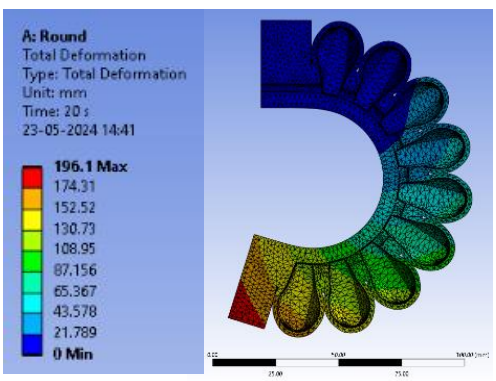

(d)

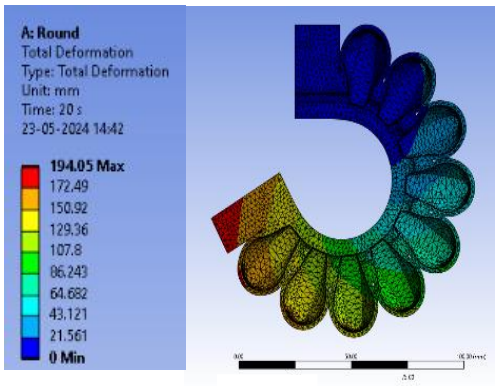

(e)

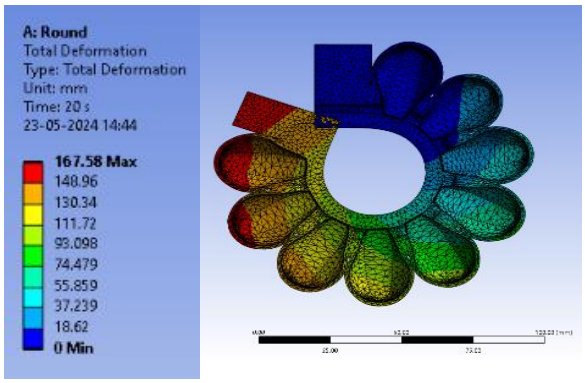

(f)

Fig.4.13. Total deformation at different pressures in Dragon skin-0030 with half round geometry. (a) At 30 kPa, (b) At 40 kPa, (c) At 50 kPa, (d) At 60kPa, (e) At 70 kPa

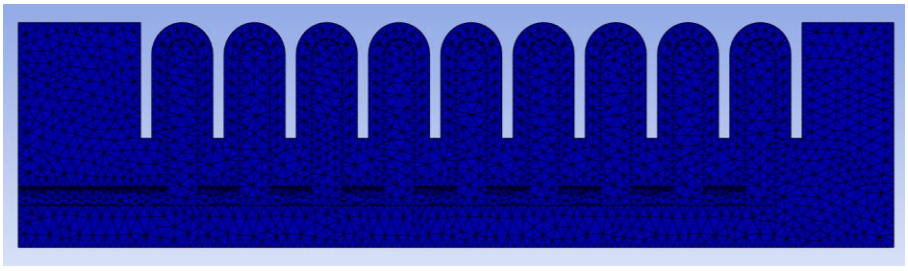

(a)

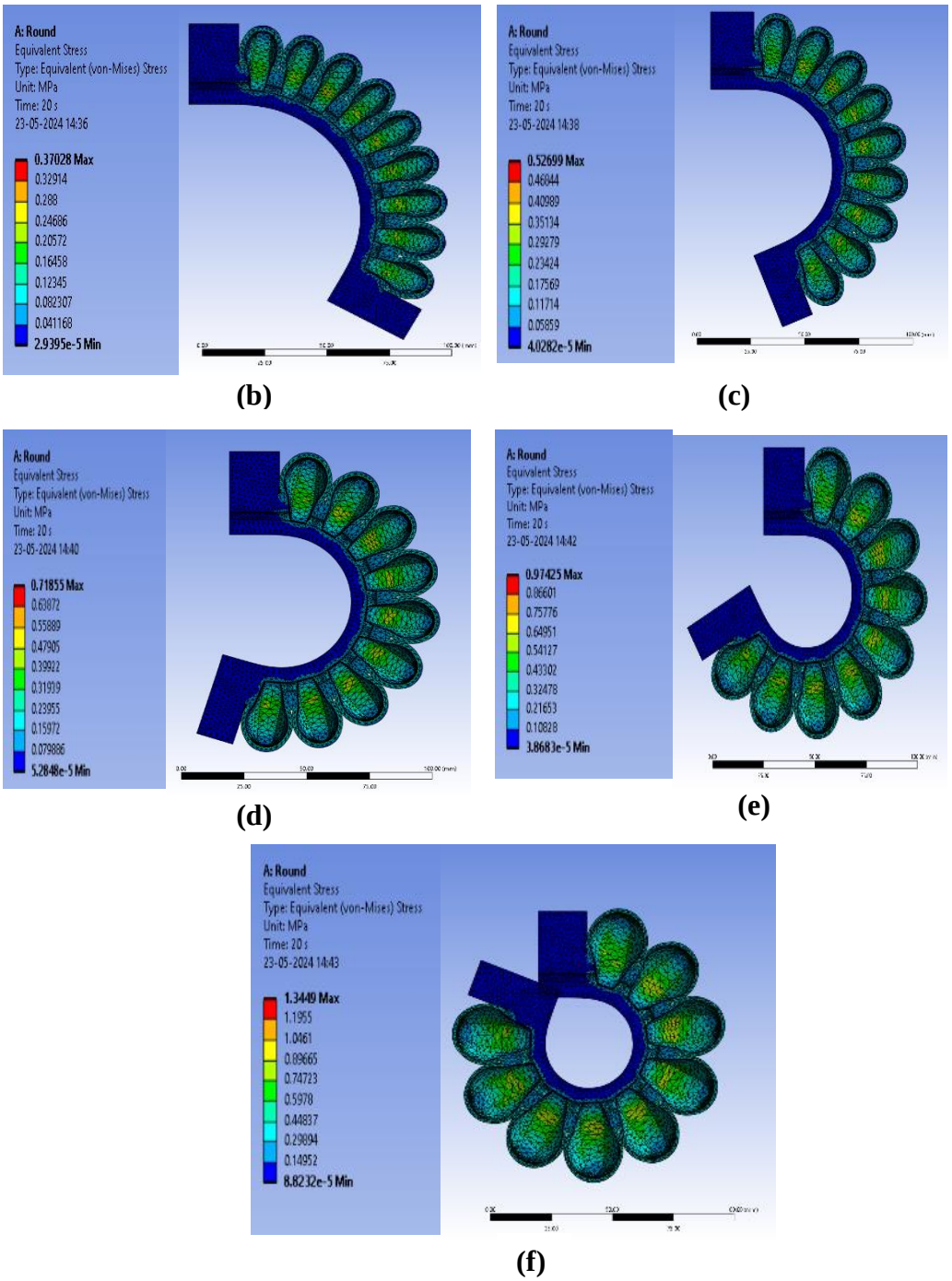

Fig.4.14. Equivalent stress at different pressures in dragon skin-0030 with half round geometry. (a) At 30 kPa, (b) At 40 kPa, (c) At 50 kPa, (d) At 60 kPa, (e) At 70 kPa

Table 4.8 parameterisation of dragon skin-0030 with half round geometry

Sl. No.	Pressure (kPa)	Bending Angle (degree)	Equivalent Stress Maximum (kPa)
1	30	120º	370.28
2	40	158º	526.99
3	50	197º	718.55
4	60	241º	974.25
5	70	290º	1344.90

From the fig. 4.13, it is observed that the bending angles varying for each pressure were 120, 158, 197, 241, and 290 degrees. And from the fig. 4.14 it is found that the equivalent stress for different pressure ranges were 370.28, 526.99, 718.55, 974.25, and 1344.90 kPa.

Increased pressure leads to more bending, which in turn causes the material to experience higher stress. The curved surface stretches on the convex side and compresses on the concave side as it bends, creating these internal stresses. The pressure acts uniformly across the entire contact area of the half-round gripper in contact with the pressure source. However, the curved geometry leads to a non-uniform distribution of stress within the material. As the pressure and resulting internal stress increase, the bending moment eventually overcomes the material's stiffness, causing the gripper to bend. The relationship between pressure, stress, and bending angle is not perfectly linear, especially at higher pressures where material properties like stiffness play a larger role.

4.4.3.2 Dragon skin-0030 with rectangle geometry

The number of elements and nodes obtained are 45952 and 12924 respectively. For optimisation, rectangle geometry and the material dragonskin-0030 were used in the simulation. 30 kPa, 40 kPa, 50 kPa, 60 kPa and 70 kPa of pressure were applied. Corresponding bending angle and equivalent stress in

different pressure range is shown in fig. 4.15 and fig. 4.16 respectively. Results of parameterisation is shown in Table 4.9.

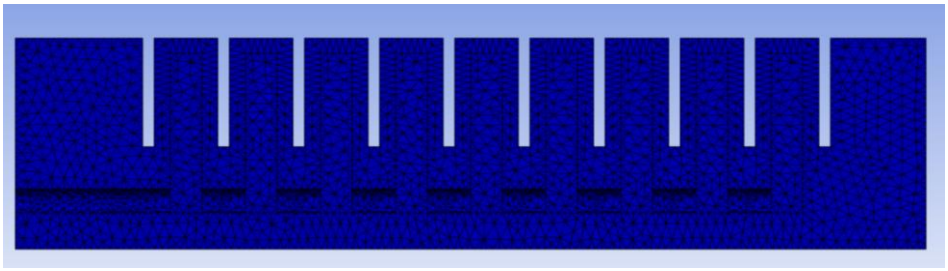

(a)

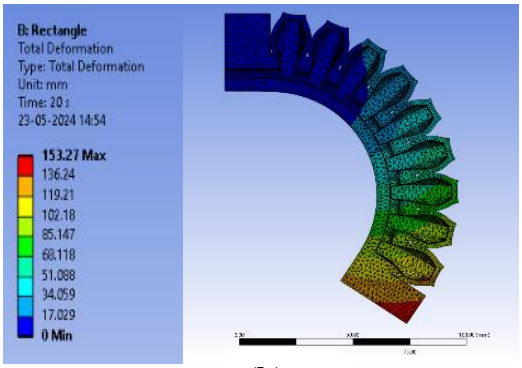

(b)

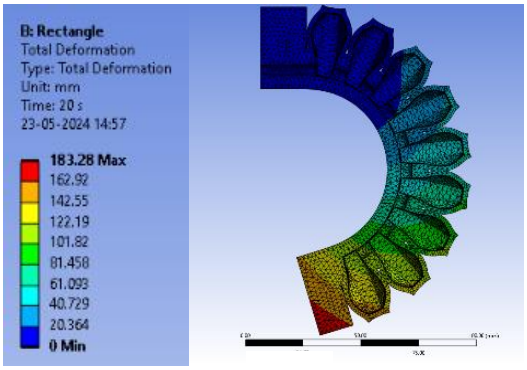

(c)

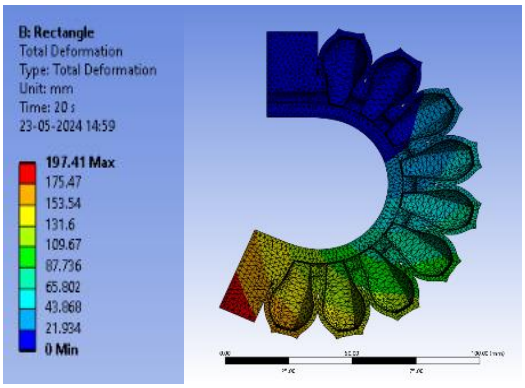

(d)

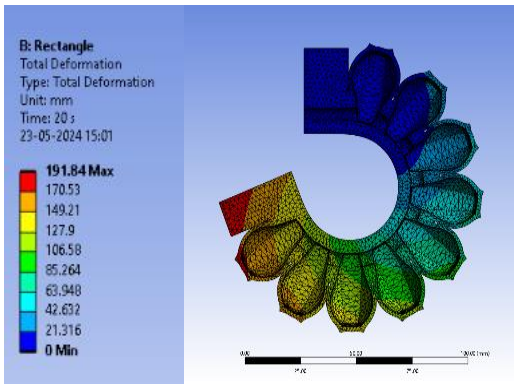

(e)

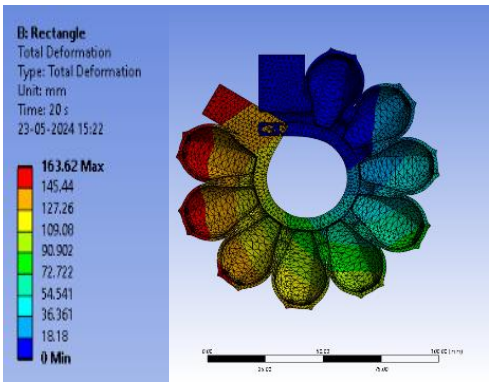

(f)

Fig.4.15. Total deformation at different pressures in dragon skin-0030 with rectangle geometry. (a) At No pressure (b) At 30 kPa, (c) At 40 kPa, (d) At 50 kPa, (e) At 60 kPa, (f) At 70 kPa.

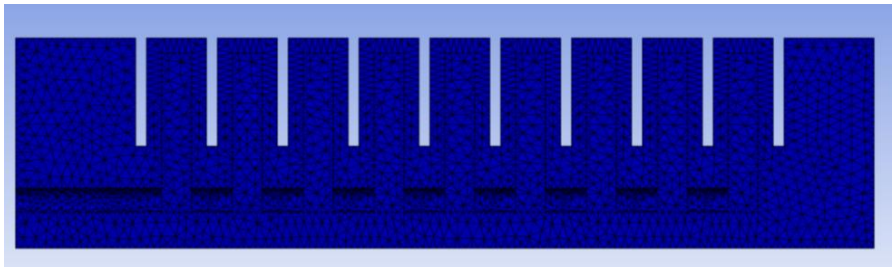

(a)

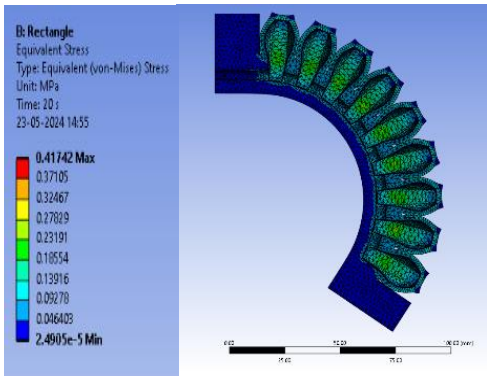

(b)

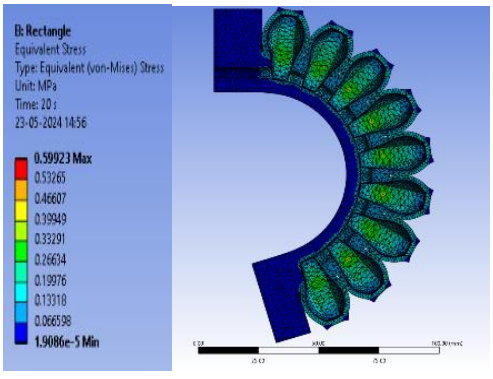

(c)

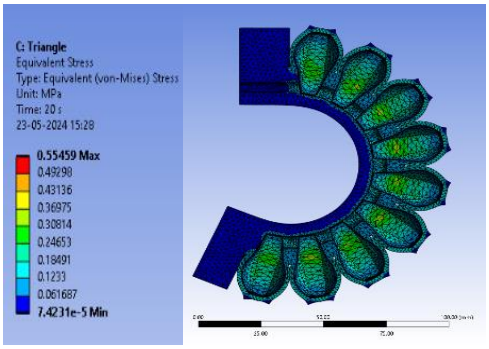

(d)

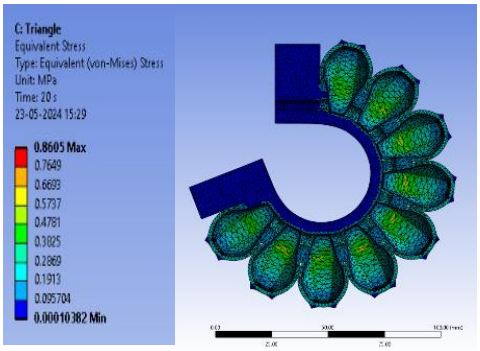

(e)

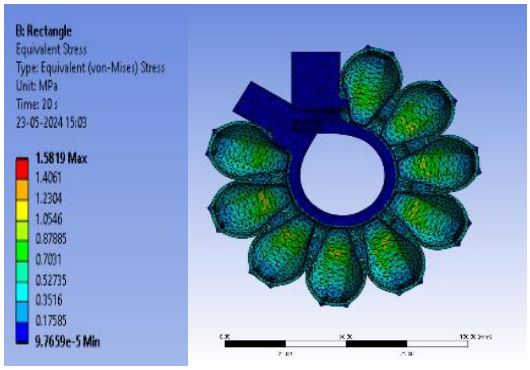

(f)

Fig.4.16 Equivalent stress at different pressures in dragon skin-0030 with rectangle geometry. (a) At No pressure (b) At 30 kPa, (c) At 40 kPa, (d) At 50 kPa, (e) At 60 kPa, (f) At 70 kPa

Table 4.9 parameterisation of dragon skin-0030 with rectangle geometry

Sl. No.	Pressure (kPa)	Bending Angle (degree)	Equivalent Stress Maximum (kPa)
1	30	124º	417.42
2	40	162.5º	599.23
3	50	204º	816.47
4	60	248º	1124.00
5	70	301º	1581.90

From the fig. 4.15, it is observed that the bending angles achieved were 124, 162.5, 204, 248, and 301 degrees at pressures of 30, 40, 50, 60, and 70 kPa. And from the fig. 4.16 it is found that the equivalent stress for different pressure ranges were 417.42, 599.23, 816.47, 1124.00 and 1581.90 kPa which showed more bending than round.

The rectangular shape of a DragonSkin-0030 significantly impacts its deflection behavior compared to half round geometry. Rectangles have a flat surface for pressure to act on, creating a concentrated bending moment that causes the finger to curve inwards. This, in contrast to half round where pressure is distributed around the circumference, leads to potentially greater deflection, especially at the center of the rectangle. The width and thickness of the rectangle directly affect its stiffness. Wider rectangles are more rigid and deflect less than narrow ones under similar pressure. Similarly, thicker rectangles will resist bending more than thinner ones.

Sharp corners of rectangles can become stress concentration points. These areas might experience slightly more localized deformation compared to a curved surface like a round finger.

4.4.3.3 Dragon skin-0030 with triangle geometry

The number of elements and nodes obtained are 42718 and 12042 respectively. For optimisation, triangle geometry and the material dragonskin-0030 were used in the simulation. 30 kPa, 40 kPa, 50 kPa, 60 kPa and 70 kPa of pressure were applied. Corresponding bending angle and equivalent stress in different pressure range is shown in fig. 4.17 and fig. 4.18 respectively. Results of parameterisation is shown in Table 4.10.

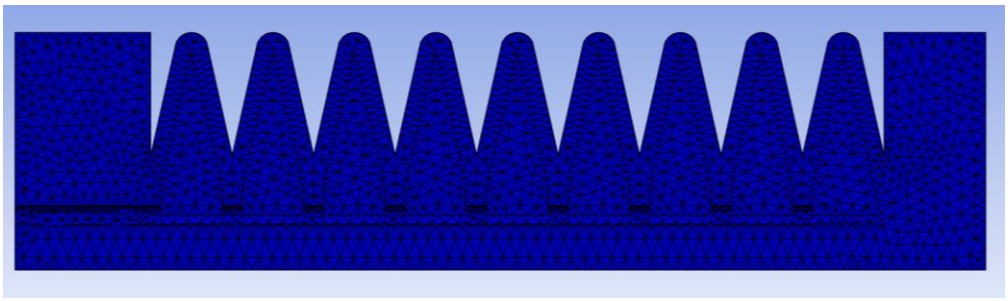

(a)

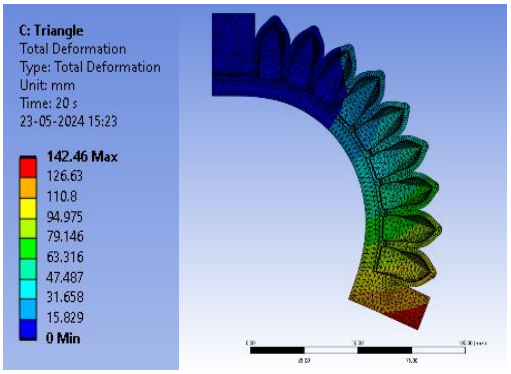
C: Triangle
Total Deformation
Type: Total Deformation
Unit: mm
Time: 20 s
23-05-2024 15:23
142.46 Max
126.63
110.8
94.975
79.146
63.316
47.487
31.658
15.829
0 Min

(b)

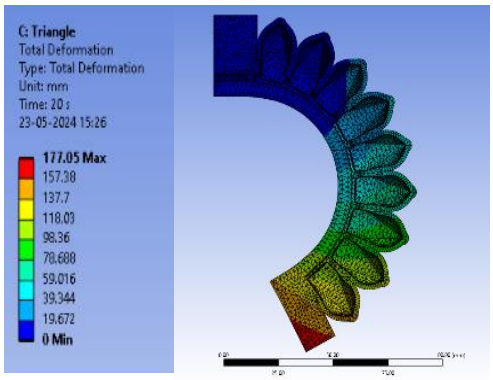
C: Triangle
Total Deformation
Type: Total Deformation
Unit: mm
Time: 20 s
23-05-2024 15:26
177.05 Max
157.38
137.7
118.03
98.36
78.688
59.016
39.344
19.672
0 Min

(c)

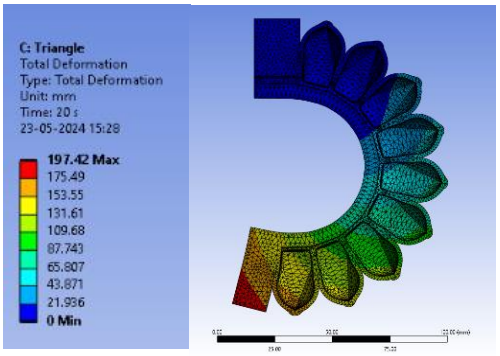
C: Triangle
Total Deformation
Type: Total Deformation
Unit: mm
Time: 20 s
23-05-2024 15:28
197.42 Max
175.49
153.55
131.61
109.68
87.743
65.807
43.871
21.936
0 Min

(c)

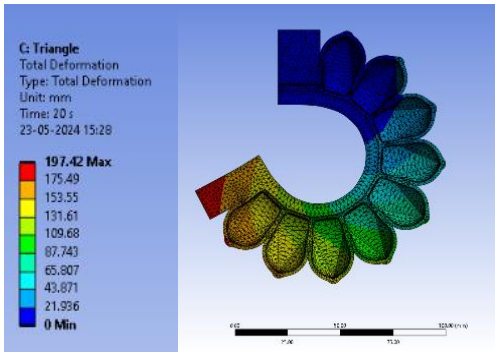
C: Triangle
Total Deformation
Type: Total Deformation
Unit: mm
Time: 20 s
23-05-2024 15:28
197.42 Max
175.49
153.55
131.61
109.68
87.743
65.807
43.871
21.936
0 Min

(d)

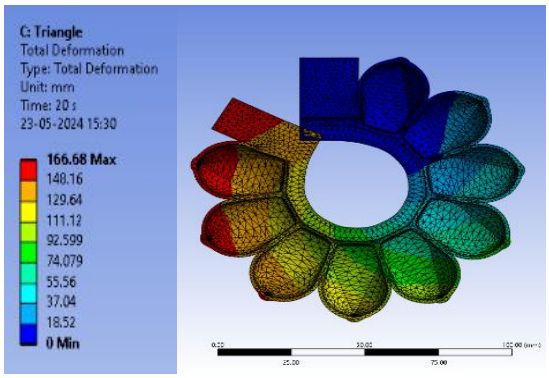

(f)

Fig.4.17. Total deformation at different pressures in dragon skin-0030 with triangle geometry. (a) At No pressure (b) At 30 kPa, (c) At 40 kPa, (d) At 50 kPa, (e) At 60 kPa, (f) At 70 kPa

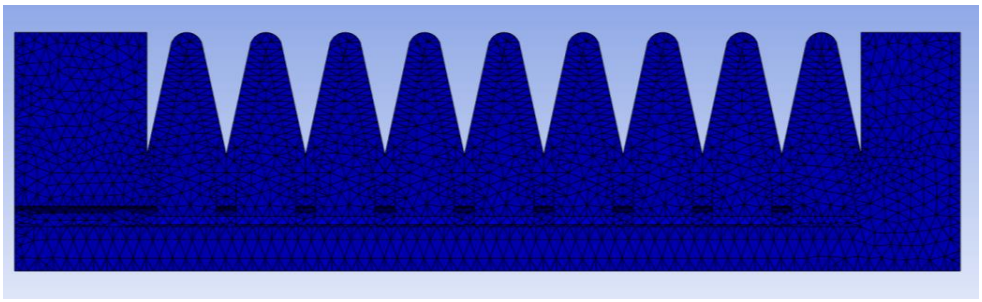

(a)

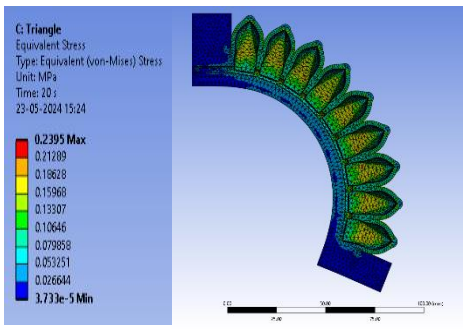

(b)

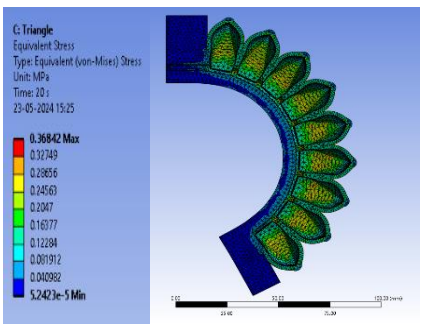

(c)

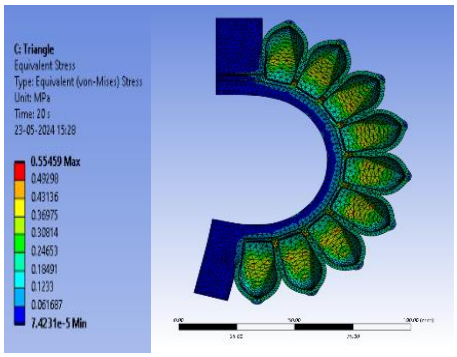

(d)

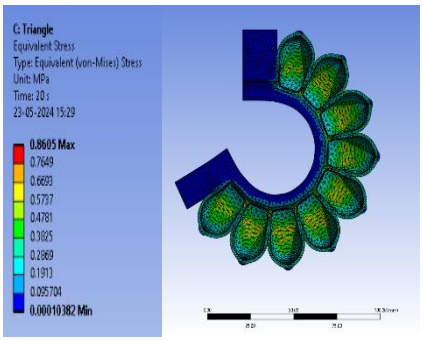

(e)

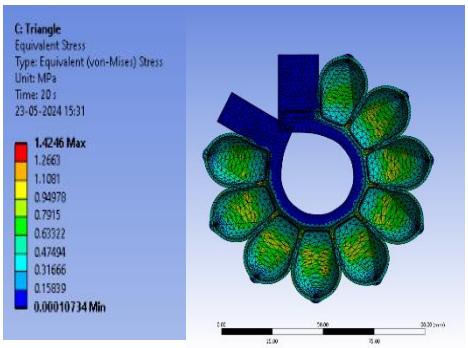

(f)

Fig.4.18 Equivalent stress at different pressures in dragon skin-0030 with triangle geometry. (a) At No pressure (b) At 30 kPa, (c) At 40 kPa, (d) At 50 kPa, (e) At 60 kPa, (f) At 70 kPa

Table 4.10 parameterisation of dragon skin-0030 with triangle geometry

Sl. No.	Pressure (kPa)	Bending Angle (degree)	Equivalent Stress Maximum (kPa)
1	30	113º	239.50
2	40	152º	368.42
3	50	198º	554.59
4	60	241º	860.50
5	70	298º	424.60

The triangle geometry exhibited greater resemblance to the rectangle geometry when subjected to the same pressures. From the fig. 4.17, it is observed

that the obtained bending angles were 113, 152, 198, 241 and 298 degrees for different pressure ranges. The corresponding equivalent stresses were 239.50, 368.42, 554.59, 860.50 and 424.60kPa for different pressure ranges shown in fig. 4.18.

Triangle shaped DragonSkin-0030 gripper offer interesting trade-offs compared to rectangles and half round geometry. Unlike rectangles, triangles excel in resisting bending in a specific direction. This allows to align the triangle's stiffest axis with the gripping force, achieving more controlled deflection. Additionally, triangles can potentially be lighter than rectangles with similar rigidity, benefiting applications where weight is a concern. Sharp corners, like in rectangles, can become stress concentration points, potentially causing slightly higher localized deformation.

Out of the three materials used in the study, Dragonskin 30 has relatively medium stiffness, which explains how it gives higher bending angle before the smoothsil pressure range. This is because stiffer materials offer greater resistance to deformation. With the same amount of air pressure pushing outwards, a stiffer material will bend less compared to a softer material. Actuation in geometry is in similar ways as mentioned earlier.

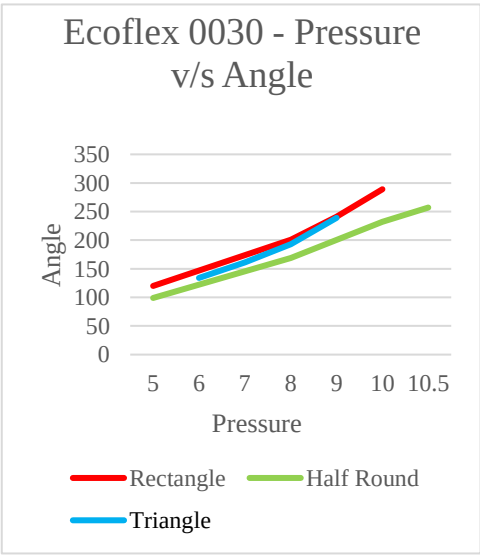

(a)

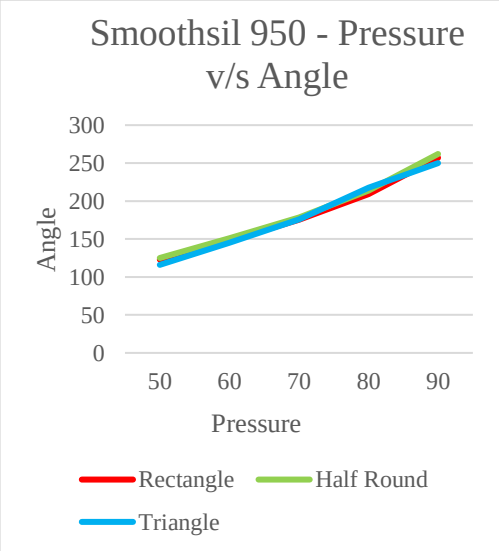

(b)

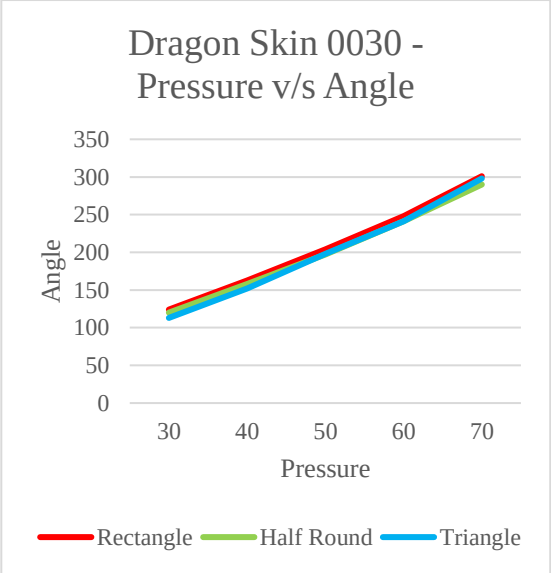

(c)

Fig.4.19 Pressure v/s Angle graph: (a) Dragon skin 0030 (b) Ecoflex 0030 (c) Smoothsil- 950

Rectangle has highest bending in low pressure and triangle shows comparatively low bending angle in low pressure and almost reaching similar bending angle in high pressure. Half round geometry has less bending angle than rectangle and high bending angle than triangle upto a particular pressure. There for we can say rectangle has better property for the material dragon skin 0030.

Rectangle has highest bending in low pressure and triangle shows comparatively low bending angle in low pressure and almost reaching similar bending angle in high pressure. Half round geometry has less bending angle than triangle. There for we can say rectangle has better property for the material ecoflex 0030.

Half round has highest bending in low pressure and rectangle shows comparatively low bending angle in low pressure and almost reaching similar bending angle in high pressure. Triangle geometry has less bending angle than rectangle upto a pressure and it bending angle reaches above half round geometry

and reaches below rectangle after a limit of pressure. There for we can say half round has better property for the material smoothsil 950.

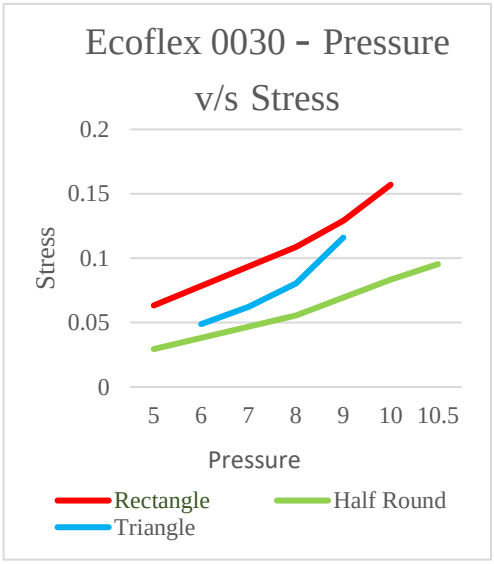

(a)

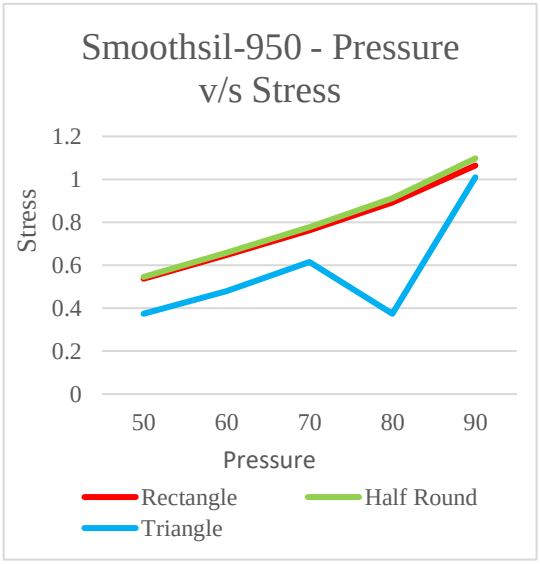

(b)

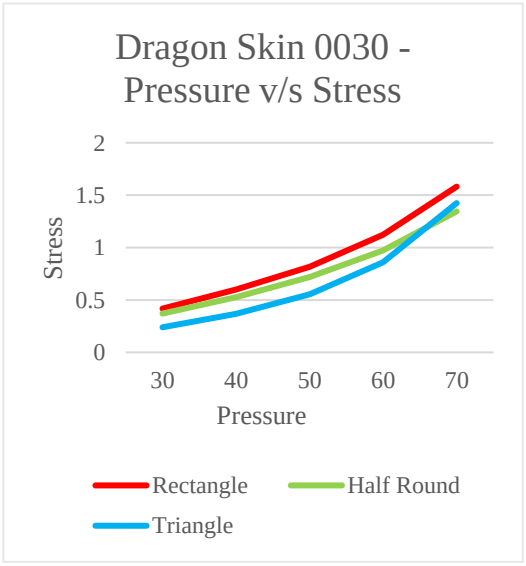

(c)

Fig.4.20 Pressure v/s Stress graph: (a) Dragon skin 0030 (b) Ecoflex 0030 (c) Smoothsil 950

When considering stress for dragon skin material, triangle geometry shows low stress in a wide range whereas, rectangle geometry has highest stress and half

round geometry comes in middle of the other two geometries but becomes lower than triangular geometry at high pressure. If we consider stress triangle geometry works better in dragon skin material.

In ecoflex material half round has lower stress, rectangle geometry showing higher and triangle geometry coming in middle of the other two. If ecoflex is used as a material considering stress half round geometry is better.

In smoothsil triangular geometry shows a varying yet lower stress at all pressures whereas other two geometries have almost similar stress in which rectangle geometry shows a small deviation as the pressure increase.

The firmness of pineapple was obtained from the texture analyzer data of compression test. Compression test was done at two positions, top and bottom of each pineapple. The average firmness of the pineapple was obtained as 3.75N.cm^{-2} (ie; 37.50 kPa). From these we can conclude that the maximum pressure to hold pineapple without damage is 37.50 kPa. Minimum pressure required to hold pineapple against gravity is 30 kPa. There for the optimum pressure required to hold pineapple is 30-40 kPa. After considering all the losses in the chamber, it is concluded that the pressure range required to hold the pineapple by gripper is (30-40) × 1.5 = 45-60 kPa

Here, the maximum pressure range withstand by Ecoflex-0030 with all geometry is 10.50 kPa. So it couldn't use as material for pineapple soft gripper. Whereas the pressure range of Smoothsil-950 & Dragon-0030 is in between (50-90 kPa) & (30-70 kPa) respectively.

Based on the obtained simulation results, it is observed that a soft gripper fabricated with Dragon Skin 30 and smoothsil 950 hyper-elastic materials are coming under the required pressure needed to hold pineapple without any damage. The maximum bending angle of Smoothsil-950 and Dragonskin-0030 for rectangle geometry at 50 kPa is 123 & 204 degree respectively. Here dragonskin-0030 have more bending than smoothsil-950. So, dragonskin-0030 is the most suitable material for fabrication.

For the geometry optimisation, three geometries (Triangle, rectangle and half round) are taken. Obtained bending angle for triangle, rectangle & half round geometries are 198º, 204º and 197º respectively. Among the three geometries, the rectangle geometry shows maximum deformation (204º) for dragon skin-0030 under 50 kPa.

The maximum equivalent stress occurred on the triangle, rectangle & half round geometries are 554.50 kPa, 816.40 kPa and 718.50 kPa respectively. Among these geometries, triangle geometry have the least stress. While considering these two parameters (bending angle and equivalent stress) for optimisation, the small difference in bending angle (6º) won't affect much on gripping of pineapple, but the slight difference in equivalent stress (0.30 MPa) may have significant effect on the gripper while doing repeated operations.

Summary and conclusion

CHAPTER V

SUMMARY AND CONCLUSION

Nowadays, harvesting delicate and high-value fruits, vegetables, and edible fungi requires a large input of manual human labour. The relatively low wages and many health problems the workforce faces make this profession increasingly unpopular. Meanwhile, robotic systems that selectively harvest crops are being developed. Robotic grippers serve as the fundamental "hand" of robots, providing critical grasping and manipulation functions. Typically, these grippers employ mechanical, electrical, or other power sources to switch between grasping and releasing modes. To execute successful grasps, robotic grippers must exhibit precision in their gripping actions to prevent slippage and damage, as well as adapt their grasping strategies spontaneously based on the object characteristics. While rigid robots excel in executing repetitive tasks along assembly lines, their interactions with delicate objects remain a safety concern due to the lack of flexibility in their links, joints, and structures. Therefore it paved the way for the development of soft robotic grippers.

Soft grippers are specially designed grippers with soft material which is used to pick up objects, especially fruits, very gently so that no damage is caused to the fruit. Major advantage of soft gripper is that it can safe hands fragile and delicate objects for higher production quality. Pineapple gripper can be used for gripping pineapples as pineapple harvester plucks the fruit from the plant. Moreover, it can be used for holding and grading of pineapple during its post-harvest operations as well as transportation. Thus, it is to be designed so carefully that it should not cause any damage to the fruit but still grip the fruit firmly.

Physical and mechanical properties of pineapple assessed by evaluating fruit parameters such as top, bottom, middle, transverse diameter, vertical length and weight of pineapple were 7.74, 9.53, 10.14, 16.35, 19.32 cm, 1.36 kg respectively and average firmness obtained as 37.5 kPa. Then we have designed soft gripper for pineapple harvesting using CAD software – Solidworks with

measurements 143 mm, 2.50 mm, 17 mm, 1.80 mm, 35 mm as length of gripper, wall thickness, bottom width, gap between adjacent channels and height of gripper respectively by considering 5th to 95th percentile of all the measured physical and mechanical properties.

Optimisation of soft gripper has been carried out by considering geometry (triangle, rectangle and half round), materials (Ecoflex-0030, Dragonskin 0030 and Smoothsil 950) at different pressures using finite element analysis of soft grippers with the help of ANSYS workbench R2.

From the compression test, it is found that the maximum pressure to hold pineapple without damage is 37.50 kPa. From these we can conclude that the maximum pressure to hold pineapple without damage is 37.50 kPa. Minimum pressure required to hold pineapple against gravity is 30 kPa. There for the optimum pressure required to hold pineapple is 30-40 kPa. After considering all the losses in the chamber, it is concluded that the pressure range required to hold the pineapple by gripper is 45-60 kPa.

Based on the FEA analysis it is observed that Dragon Skin 30 and smoothsil 950 hyper-elastic materials are coming under the required pressure needed to hold pineapple without any damage. The maximum bending angle of Smoothsil-950 and Dragonskin-0030 for rectangle geometry at 50 kPa is 123 & 204 degree respectively. Here dragonskin-0030 have more bending than smoothsil-950. So, dragonskin-0030 is the most suitable material for fabrication. From the three geometries (Triangle, rectangle and half round), bending angles obtained for triangle, rectangle & half round geometries are 198º, 204º and 197º respectively. Among the three geometries, the rectangle geometry shows maximum deformation (204º) for dragon skin-0030 under 50 kPa.

From the two parameters bending angle and equivalent stress for optimisation, the small difference in bending angle (6º) won't affect much on gripping of pineapple, but the slight difference in equivalent stress (0.30 MPa) may have significant effect on the gripper while doing repeated operations.

Thus, it can be concluded that out of the above stated three hyper-elastic materials and geometries, Dragon skin 30 with triangle geometry is best for fabricating soft grippers in terms of bending angle and experienced stress. For future work, similar soft grippers can be developed experimentally and their performance can be compared practically.

The developed robotic gripper works on the basis of positive pressure. There is a difficulty in opening the gripper when it reaches the pineapple. Applying negative pressure in the beginning and then reaching the pineapple can resolve the problem. Modifying the developed soft robotic gripper so that it can actuate both by positive and negative pressure will be more commendable. The dimensions of this three different geometry can also be varied and their dimensional optimisation can be done using FEM. Fatigue test can be done to predict the strength variations occurring during repeated operations. Making slight changes in the gripper designs like granular jamming in the gripper may also increase the stiffness of gripper.

References

REFERENCES

Abd, M.A., Ades, C., Shuqir, M., Holdar, M., Al-Saidi, M., Lopez, N., and Engeberg, E.D. 2017. Impacts of soft robotic actuator geometry on end effector force and displacement. In: 30th Florida Conference on Recent Advances in Robotics, May, pp. 11-12

Anh, N.P.T., Hoang, S., Van Tai, D., and Quoc, B.L.C. 2020. Developing robotic system for harvesting pineapples. In: 2020 International Conference on Advanced Mechatronic Systems (ICAMechS), pp. 39-44. IEEE

Bernardi, L., Hopf, R., Ferrari, A., Ehret, A.E., and Mazza, E. 2017. On the large strain deformation behavior of silicone-based elastomers for biomedical applications. *Polym. Testing* 58: 189-198.

Brown, E., Rodenberg, N., Amend, J., Mozeika, A., Steltz, E., Zakin, M.R., Lipson, H., and Jaeger, H.M. 2010. Universal robotic gripper based on the jamming of granular material. *Proc. Natl. Acad. Sciences* 107(44): 18809-18814.

Cianchetti, M., Licofonte, A., Follador, M., Rogai, F., and Laschi, C. 2014. Bioinspired soft actuation system using shape memory alloys. *In: Actuators* 3(3): 226-244. MDPI

Elsayed, Y., Vincensi, A., Lekakou, C., Geng, T., Saaj, C.M., Ranzani, T., Cianchetti, M., and Menciassi, A. 2014. Finite Element Analysis and Design Optimization of a Pneumatically Actuating Silicone Module for Robotic Surgery Applications. *Soft Robot* 1: 255–262.

Gariya, N. and Kumar, P. 2022. A comparison of plane, slow pneu-net, and fast pneu-net designs of soft pneumatic actuators based on bending behavior. *Mater. Today: Proc*. 65:3799-3805

Gariya, N., Kumar, P., Bangari, R.S. and Makkar, M., 2023. Bending analysis of a soft pneumatic actuator using analytical and numerical methods. *Materials Today: Proceedings*.

Hu, W., Mutlu, R., Li, W. and Alici, G., 2018. A structural optimisation method for a soft pneumatic actuator. *robotics*, *7*(2): 24.

Jiao, Z., Zhuang, Z., Cheng, Y., Deng, X., Sun, C., Yu, Y., and Li, F. 2022. Lightweight Dual-Mode Soft Actuator Fabricated from Bellows and Foam Material. *Actuators* 11: 245.

Kerala Agricultural University 2016. Package of practices Recommendations: Crops 15th edition. Kerala Agricultural University, Thrissur-p.

Kultongkham, A., Kumnon, S., Thintawornkul, T., and Chanthasopeephan, T. 2021. The design of a force feedback soft gripper for tomato harvesting. *J. Agric. Eng.* 52(1).

Lei, J., Ge, Z., Fan, P., Zou, W., Jiang, T., and Dong, L. 2022. Design and Manufacture of a Flexible Pneumatic Soft Gripper. *Appl. Sciences* 12(13): 6306

Li, Y., Chen, Y., Ren, T., Y., and Choi, S.H. 2018. Precharged pneumatic soft actuators and their applications to untethered soft robots. *Soft Robotics* 5(5): 567-575.

Manti, M., Hassan, T., Passetti, G., D'Elia, N., Laschi, C., and Cianchetti, M. 2015. A bioinspired soft robotic gripper for adaptable and effective grasping. *Soft Robotics* 2(3): 107-116

Mosadegh, B., Polygerinos, P., Keplinger, C., Wennstedt, S., Shepherd, R.F., Gupta, U., Shim, J., Bertoldi, K., Walsh, C.J., and Whitesides, G.M. 2014. Pneumatic networks for soft robotics that actuate rapidly. *Advanced Funct. Mater.* 24(15): 2163-2170

Navas, E., Fernández, R., Sepúlveda, D., Armada, M. and Gonzalez-de-Santos, P., 2021. Soft grippers for automatic crop harvesting: A review. *Sensors*, *21*(8): 2689.

Navas, E., Fernandez, R., Sepulveda, D., Armada, M., and Gonzalez-de-Santos, P. 2021a. Soft Gripper for Robotic Harvesting in Precision Agriculture Applications. In: 2021 IEEE International Conference on Autonomous Robot Systems and Competitions (ICARSC), IEEE, Santa Maria da Feira, 111 Portugal, pp. 167–172.

Navas, E., Shamshiri, R.R., Dworak, V., Weltzien, C. and Fernández, R., 2024. Soft gripper for small fruits harvesting and pick and place operations. *Frontiers in Robotics and AI*, 10, p.1330496.

Ongaro, F., Scheggi, S., Yoon, C., den Brink, F.V., Oh, S.H., Gracias, D.H., and Misra, S. 2017. Autonomous planning and control of soft untethered grippers in unstructured environments. *J. Micro-bio Robotics* 12(1): 45-52.

Pathaveerat, S., Terdwongworakul, A., and Phaungsombut, A. 2008. Multivariate data analysis for classification of pineapple maturity. *J. Food Eng*. 89(2): 112-118.

Razif, M.R.M., Zhi, G.L., Nordin, I.N.A.M., Hashim, H., Sadun, A.S., and Rehman, T. 2020. Bellow soft gripper for agriculture. *Int. J. Advanced Trends Comput. Sci. Eng*. 9(1.4)

Riady, S, J. and Evans, N. 2024. Parametric study of soft pneumatic robot grippers through finite element analysis. Int. J. of Robotics and Automation. 13(1):19-30.

Salleh, N.F.M. and Sukadarin, E.H. 2018. Defining human factor and ergonomic and its related issues in malaysia pineapple plantations. *MATEC Web Conf*. 150: 05047

Saloni, S., Chauhan, K. and Tiwari, S. 2017. Pineapple production and processing in north eastern India. *Journal of Pharmacognosy and Phytochemistry*, *6*(6S), pp.665-672.

Shintake, J., Cacucciolo, V., Floreano, D., and Shea, H. 2018. Soft robotic grippers. *Advanced mater*. 30(29): 1-33.

Shiva, A., Stilli, A., Noh, Y., Faragasso, A., De Falco, I., Gerboni, G., Cianchetti, M., Menciassi, A., Althoefer, K., and Wurdemann, H.A. 2016. Tendonbased stiffening for a pneumatically actuated soft manipulator. *IEEE Robotics Automation Lett*. 1(2): 1-6.

Sinatra, N.R., Teeple, C.B., Vogt, D.M., Parker, K.K., Gruber, D.F., and Wood, R.J. 2019. Ultragentle manipulation of delicate structures using a soft robotic gripper. *Sci. Robotics* 4(33): 5425.

Singh, H.J. 2020. Progress on research & development in pineapple harvesting: special emphasis on Indian scenario. *Sci. Cult*. 86: 178-187

Singh, M.A., Lande, S.D., Mishra, I.M., Prakash, J., Khura, T.K.K. and Sarkar, S.K., 2022. Semi-automatic pineapple harvester for mechanization of pineapple harvesting in North East Hill (NEH) regions of India.

Terrile, S., Argüelles, M., and Barrientos, A. 2021. Comparison of Different Technologies for Soft Robotics Grippers. *Sensors* 21: 3253.

Terryn, S., Brancart, J., Lefeber, D., Van Assche, G., and Vanderborght, B. 2017. Self-healing soft pneumatic robots. *Sci. Robot* 2: 4268.

Thomas, L. and Dinesh, V. 2020. Economics of pineapple cultivation under climate variability in kerala, INDIA. *Plant Arch*. 20(2): 3292-3295

Tolley, M.T., Shepherd, R.F., Mosadegh, B., Galloway, K.C., Wehner, M., Karpelson, M., Wood, R.J., and Whitesides, G.M. 2014. A Resilient, Untethered Soft Robot. *Soft Robot* 1: 213–223.

Valente, M., Duprat, F., Grotte, M., and Lasaygues, P. 2001. Non-destructive evaluation of firmness of fresh pineapple by acoustic method. *Acta Hortic*. pp. 391-396.

Wang, H., Li, B., Liu, G., and Xu, L. 2012. Design and test of pineapple harvesting manipulator. *Trans. Chinese Soc. Agric. Eng*. 28(1): 42-46

Wang, X., Kang, H., Zhou, H., Au, W., Wang, M.Y. and Chen, C., 2023. Development and evaluation of a robust soft robotic gripper for apple harvesting. *Computers and Electronics in Agriculture*, *204*, p.107552.

Wang, Z. and Hirai, S. 2016. A 3D printed soft gripper integrated with curvature sensor for studying soft grasping. In: 2016 IEEE/SICE *International Symposium on System Integration (SII)*, pp. 629-633. IEEE

Xia, H., Li, Q., and Zhen, W. 2012. Design of a pineapple picking end actuator. *Appl. Mech. Mater*. 184-185: 134-139.

Xiao, W., Liu, C., Hu, D., Yang, G. and Han, X., 2022. Soft robotic surface enhances the grasping adaptability and reliability of pneumatic grippers. *International Journal of Mechanical Sciences*, *219*, p.107094.

Zaidi, S., Maselli, M., Laschi, C., and Cianchetti, M. 2021. Actuation Technologies for Soft Robot Grippers and Manipulators: *A Review. Curr. Robotics Rep*. 2: 355–369

Zhang, L., Tang, S., Li, P., Cui, S., Guo, H., and Wang, F. 2018. Structure design of a semi-automatic pineapple picking machine. *Mater. Sci. Eng*. 452: 042155

Zhu, M., Mori, Y., Wakayama, T., Wada, A., and Kawamura, S. 2019. A fully multi-material three-dimensional printed soft gripper with variable stiffness for robust grasping. *Soft Robotics* 6(4): 507-519

FINITE ELEMENT ANALYSIS OF SOFT ROBOTIC GRIPPER FOR PINEAPPLE HARVESTING

BY

SUMITH S RAJU (2020-02-014)

JUSTIN BASIL ISAC (2020-02-019)

SOORYA SURENDRAN (2020-02-025)

AFNA SHARIN E P (2020-02-031)

ABSTRACT

Submitted in partial fulfillment of the requirement for the degree of Bachelor of Technology

in

Agricultural Engineering

Faculty of Agricultural Engineering and Technology

KERALA AGRICULTURAL UNIVERSITY

DEPARTMENT OF FARM MACHINERY AND POWER ENGINEERING

KELAPPAJI COLLEGE OF AGRICULTURAL ENGINEERING AND TECHNOLOGY

TAVANUR-679573, MALAPPURAM

KERALA , INDIA

2024

ABSTRACT

Nowadays, harvesting delicate and high-value fruits, vegetables, and edible fungi requires a large input of manual human labour. Robotic systems that selectively harvest crops are being developed. Robotic grippers serve as the fundamental “hand” of robots, providing critical grasping and manipulation functions. Typically, these grippers employ mechanical, electrical, or other power sources to switch between grasping and releasing modes. To execute successful grasps, robotic grippers must exhibit precision in their gripping actions to prevent slippage and damage, as well as adapt their grasping strategies spontaneously based on the object characteristics. While rigid robots excel in executing repetitive tasks along assembly lines, their interactions with delicate objects remain a safety concern due to the lack of flexibility in their links, joints, and structures. Therefore it paved the way for the development of soft robotic grippers.

The project has been carried out to develop a soft robotic pineapple gripper with the following objectives. To study fruit parameters towards the development of soft robotic pineapple grippers, to design soft robotic pineapple gripper and the geometry and material optimisation of soft robotic pineapple gripper.

Physical and mechanical properties of pineapple assessed by evaluating fruit parameters such as shape, size, length, diameters, weight and firmness which were then used for the design of soft robotic pineapple gripper. Soft robotic pineapple gripper was designed by considering 5th to 95th percentile of all the measured physical and mechanical properties. Soft gripper has been developed using design/ CAD software – SolidWorks. Optimisation of soft gripper has been carried out by considering geometry (triangle, rectangle and half round), materials (Ecoflex-0030, Dragonskin 0030 and Smoothsil 950) at different pressures using finite element analysis of soft grippers with the help of ANSYS workbench R2. From the three hyper-elastic materials and geometries, Dragon skin 30 with triangle geometry is best for fabricating soft grippers in terms of bending angle and experienced stress. For future work, similar soft grippers can be developed experimentally and their performance can be compared practically.